Western Graduate&PostdoctoralStudies

Western University
Scholarship@Western

Electronic Thesis and Dissertation Repository

8-11-2014 12:00 AM

Investigating the Multiple Hit hypothesis of Parkinson disease using transgenic LRRK2-R1441G rats

Komal T. Shaikh, *The University of Western Ontario*

Supervisor: Dr. Susanne Schmid, *The University of Western Ontario*

A thesis submitted in partial fulfillment of the requirements for the Master of Science degree in Neuroscience

© Komal T. Shaikh 2014

Follow this and additional works at: https://ir.lib.uwo.ca/etd

Part of the Behavioral Neurobiology Commons, and the Other Neuroscience and Neurobiology Commons

Recommended Citation

Shaikh, Komal T., "Investigating the Multiple Hit hypothesis of Parkinson disease using transgenic LRRK2-R1441G rats" (2014). *Electronic Thesis and Dissertation Repository*. 2333.
https://ir.lib.uwo.ca/etd/2333

This Dissertation/Thesis is brought to you for free and open access by Scholarship@Western. It has been accepted for inclusion in Electronic Thesis and Dissertation Repository by an authorized administrator of Scholarship@Western. For more information, please contact wlswadmin@uwo.ca.

INVESTIGATING THE MULTIPLE HIT HYPOTHESIS OF PARKINSON DISEASE USING TRANSGENIC LRRK2^{R1441G} RATS

(Thesis format: Monograph)

by

Komal Shaikh

Graduate Program in Neuroscience

A thesis submitted in partial fulfillment
of the requirements for the degree of
Master of Science

The School of Graduate and Postdoctoral Studies
The University of Western Ontario
London, Ontario, Canada

© Komal Shaikh 2014

Abstract

The ‘multiple hit’ hypothesis of Parkinson disease (PD) suggests that the combination of several risk factors leads to the development of PD. Here, we explore the interaction between two potential causes of PD; a genetic mutation in the leucine-rich repeat kinase 2 (*LRRK2)* gene and exposure to the neurotoxin, Paraquat. This project characterizes transgenic BAC rats expressing human *LRRK2* bearing the familial PD mutation, R1441G. These rats were tested for PD-related deficits at 3, 6, 9 & 12 months. These rats were then exposed to intraperitoneal injections of Paraquat. We hypothesized that *LRRK2*^{R1441G} rats will show increased vulnerability to Paraquat compared to wildtype controls. Our results showed that *LRRK2*^{R1441G} rats are not significantly different from wildtype rats by the 12 month stage, suggesting that this mutation alone is insufficient to manifest PD-like features in rats. In addition *LRRK2*^{R1441G} rats failed to show increased vulnerability to Paraquat administration.

Keywords

Parkinson disease, leucine-rich repeat kinase 2, genetic model, transgenic BAC rats, motor test, cognitive assessment, ‘multiple hit’ hypothesis, Paraquat

Acknowledgements

I would like to thank my supervisor, Dr. Susanne Schmid for introducing me to lab work and for her support and guidance throughout the years. In addition, thank you to all members of the Schmid Lab who got me through bad science days.

Dedications

I would like to dedicate this work to my loving family. To Tariq, who thinks Neuroscience is fine but suggests I take up a ‘real’ job, such as engineering. To Bushra, who is glad I’m getting work done but still wants to make sure I’m eating properly. To Hannah, who does not want to hear about disgusting rats. And finally, to Umar, who is pretty sure I’m faking the whole grad school thing anyway.

Table of Contents

Abstract ii

Acknowledgements iii

Dedications iii

Table of Contents iv

List of Tables vi

List of Figures vii

Chapter 1 10

1.1 Introduction 10

Chapter 2 12

2 Literature Review 12

2.1 Parkinson Disease 12

2.2 LRRK2: molecular structure, physiological role, and distribution 15

2.3 PD Related LRRK2 Mutations 18

2.4 Genetic LRRK2 Animal Models 19

2.5 Mechanisms of LRRK2-mediated neurodegeneration 20

2.6 Environmental Toxins and PD 22

2.7 Multiple Hit Hypothesis 23

Chapter 3 27

3 Research Purpose and Hypotheses 27

Chapter 4 28

4 Materials and Methods 28

4.1 Study 1: Assessing PD-related phenotypes in *LRRK2*^{R1441G} transgenic rats 28

4.1.1 Animals 28

4.1.2 Genotyping 28

4.1.3 Behavioral Testing 29
4.2 Study 2: Testing Paraquat Vulnerability in aged *LRRK2*^{R1441G} transgenic rats 32
4.2.1 Vulnerability to Paraquat 32
4.2.2 q-RT PCR 32
4.2.3 Statistical Analysis 33
Chapter 5 34
5 Results 34
5.1 Study 1: Assessing PD-related phenotypes in *LRRK2*^{R1441G} transgenic rats 34
5.1.1 Motor Tests 35
5.1.2 Cognitive Tests 41
5.2 Study 2: Testing Paraquat Vulnerability in aged *LRRK2*^{R1441G} transgenic rats 65
Chapter 6 73
6 Discussion 73
6.1 Introduction 73
6.2 Evidence from other transgenic models of LRRK2 mediated PD 73
6.3 Limitations of the Model 74
6.4 Multiple Hit Hypothesis of PD 75
6.5 Methodological Considerations 76
6.6 Summary of findings 77
References 79
Curriculum Vitae 94

List of Tables

Table 1: qRT-PCR expression of wildtype and transgenic animals. 72

List of Figures

Figure 1: Progression of Parkinson disease. 14

Figure 2: LRRK2 Structure. 17

Figure 3: Multiple factors affect PD. 26

Figure 4: Rat Weight. 34

Figure 5: Vibrissae Evoked Forelimb Placing. 35

Figure 6: Adjusting Steps Task. 36

Figure 7: Stride Length. 37

Figure 8: Total distance travelled in open field test. 39

Figure 9: Rearing behavior in open field test. 40

Figure 10: Maximal velocity in open field test. 41

Figure 11: Baseline startle amplitude. 43

Figure 12: Habituation of the acoustic startle response. 44

Figure 13: Habitation of the acoustic startle response at 3 months of age. 45

Figure 14: Habitation of the acoustic startle response at 6 months of age. 46

Figure 15: Habitation of the acoustic startle response at 9 months of age. 47

Figure 16: Habitation of the acoustic startle response at 12 months of age. 48

Figure 17: Prepulse inhibition of the acoustic startle response with 75 dB prepulse at 3 months of age. 49

Figure 18: Prepulse inhibition of the acoustic startle response with 85 dB prepulse at 3 months of age. 50

Figure 19: Prepulse inhibition of the acoustic startle response with 75 dB prepulse at 6 months of age. 51

Figure 20: Prepulse inhibition of the acoustic startle response with 85 dB prepulse at 6 months of age. 52

Figure 21: Prepulse inhibition of the acoustic startle response with 75 dB prepulse at 9 months of age. 53

Figure 22: Prepulse inhibition of the acoustic startle response with 85 dB prepulse at 9 months of age. 54

Figure 23: Prepulse inhibition of the acoustic startle response with 75 dB prepulse at 12 months of age. 55

Figure 24: Prepulse inhibition of the acoustic startle response with 85 dB prepulse at 12 months of age. 56

Figure 25: Cued Version of the Morris Water Maze task at 9 months of age. 58

Figure 26: Spatial Reference Version of the Morris Water Maze task at 9 months of age. 59

Figure 27: Working Memory Version of the Morris Water Maze task at 9 months of age. 60

Figure 28: Probe Trial in the Morris Water Maze at 9 months of age. 61

Figure 29: Cued Version of the Morris Water Maze task at 12 months of age. 62

Figure 30: Spatial Reference Version of the Morris Water Maze task at 12 months of age. 63

Figure 31: Working Memory Version of the Morris Water Maze task at 12 months of age. 64

Figure 32: Probe Trial in the Morris Water Maze at 12 months of age. 65

Figure 33: Vulnerability to acute Paraquat poisoning. 67

Figure 34: Survival curve for transgenic and wildtype rats. 68

Figure 35: Genotype results for wildtype and transgenic animals. 69

Chapter 1

1.1 Introduction

Parkinson disease (PD), the second most common neurodegenerative disease, is characterized by the degeneration of dopaminergic neurons in the substantia nigra pars compacta (SNpc) and the presence of proteinaceous inclusions, known as Lewy bodies. Diagnosis of PD is based on distinctive motor features including resting tremor, rigidity, bradykinesia and abnormal gait. Cardinal motor features occur relatively late in the time course of the disease and by this time 60% of dopaminergic neurons have degenerated and striatal dopamine (DA) content has been reduced by 80% (Bernheimer et al., 1973). Although, PD is primarily a movement disorder, a series of nonmotor symptoms are also associated with the disease and can precede motor symptoms by several years (Chen et al., 2013). These symptoms can include loss of smell, sleep disorders, and constipation. In addition, PD patients may present with cognitive symptoms, including depression, anxiety and impaired memory (Emre, 2004).

Although the aetiology of Parkinson disease is not yet known, both genetic and environmental factors have been shown to play a role in disease development. While most cases of PD are sporadic, 5-10% are caused by familial mutations. Recently, the mapping of 16 PD associated loci (*PARK 1-16),* and the discovery of several corresponding genes has prompted renewed interest in genetic underpinnings of this disease. Mutations in the *LRRK2* gene are a common cause of familial PD and result in *PARK8* type of Parkinson disease (Paisan-Ruiz et al., 2004; Zimprich et al., 2004). *LRRK2* encodes leucine-rich-repeat kinase II, a large multidomain protein with both kinase and GTPases enzymatic functions (Zimprich et al., 2004; Santpere and Ferrer, 2009). The R1441G mutation on *LRRK2* is the second most common mutation and it increases kinase activity through modulation of GTPase activity (Healy et al., 2008). *LRRK2* mutations cause a familial PD which is indistinguishable from sporadic PD suggesting similar underlying mechanisms.

Exposure to environmental toxins, particularly agrochemicals, has also been linked to PD, underscoring the complex aetiology of this disease. In particular, exposure to *N,N'*-

dimethyl-4-4'-bipyridinium dichloride, or paraquat has been shown to increase PD risk (Costello et al., 2009). Paraquat, a widely used herbicide, induces PD related neuropathology through increased oxidative stress and production of reactive oxygen species (ROS).

The relatively low incidence of familial PD, failure to recapitulate PD phenotypes in genetic models and lack of singular environmental insult has prompted discussion that PD may not have a singular cause and instead disease phenotypes may be the outcome of multiple factors. The 'multiple hit' hypothesis of PD suggests that multiple risk factors interact to induce the degenerative process, with the primary insult causing cellular stress and all succeeding insults resulting in a loss of protective pathways which together lead to neuronal death (Sulzer, 2007).

The aim of the present study was to determine if mutated *LRRK2* would induce PD phenotypes in a rat model. We characterized transgenic BAC rats expressing human *LRRK2* bearing the autosomal dominant PD mutation, R1441G. Due to the progressive nature of PD, these rats were tested for motor and cognitive deficits, reminiscent of PD, through developmental stages of 3, 6, 9 and 12 months. As far as we are aware, this is the first study that characterizes transgenic BAC *LRRK2*^{R1441G} rats. Furthermore, in order to assess the 'multiple hit' hypothesis rats bearing the R1441G mutation were tested for vulnerability to Paraquat poisoning. We hypothesized that rats would show motor and cognitive symptoms of PD by 12 months of age and that these rats would have an increased vulnerability to Paraquat poisoning, as compared to wildtype controls.

Chapter 2

2 Literature Review

2.1 Parkinson Disease

Parkinson disease (PD), first described by James Parkinson as ‘shaking palsy,’ is the second most common neurodegenerative disease and the most common movement disorder. Like many neurodegenerative diseases, PD incidence increases with age from 0.3% in the general population to 1% in the over 60 population (Dexter and Jenner, 2013). The relative risk of developing PD is higher in males, due perhaps to estrogen’s neuroprotective properties. Although the disease manifests in slow progressive symptoms over a wide clinical spectrum, PD diagnosis is based on impaired motor function which shows responsiveness to dopaminergic medication. Classic motor features of the disease include an high amplitude, low frequency (4-7 Hz) resting tremor, rigidity, bradykinesia or slowness of movement, shuffling gait and postural instability. In addition to these motor symptoms, PD is associated with various non-motor symptoms, including sleep disorders, depression, sensory abnormalities, gastrointestinal dysfunction, sexual dysfunction and cognitive decline (Langston, 2006). The frequency of non-motor symptoms increases with disease severity and age, however, certain symptoms, including loss of smell, depression and constipation, can often precede onset of motor dysfunction (Chaudhuri et al., 2006). Cognitive impairment is common in the disease and negatively impact quality of life in patients. Patients with PD show impaired procedural and working memory, executive dysfunction, learning impairments and dementia (Williams-Gray et al., 2006).

Motor dysfunction in PD originates from degeneration of neuromelanin pigmented dopaminergic neurons in the substantia nigra pars compacta (SNpc) and subsequent dennervation of dopaminergic input from the SNpc to the striatum. Loss of striatal dopamine content accounts for many of the motor abnormalities noted in PD. Motor symptoms only occur when 60% of dopaminergic SNpc neurons have degenerated and 80% of their axon terminals have been lost (Bernheimer et al., 1973). Another characteristic feature of the disease is the presence of Lewy bodies, which are proteinaceous inclusions, composed of α-synuclein. Although neuronal loss in the SNpc

characterizes the disease, PD is associated with widespread neuropathology affecting various extranigral structures including the dorsal motor nucleus of the vagus, reticular formation, raphe nucleus, locus coeruleus, amygdala, hippocampus, and the magnocellular nuclei of the basal forebrain (Braak et al., 2003; Dexter and Jenner, 2013). In 2003, Braak and colleagues proposed a staging progression for PD-related pathology which starts in the lower brain stem (Stage I) and progresses to the pons (Stage II), the mesencephalon (Stage III), the basal prosencephalon (Stage IV) and finally to the neocoertex (Stage V and VI). This model explains the progression of PD symptoms from olfactory dysfunction early in the disease (due to damage to olfactory bulb in Stage I), to motor dysfunction (due to damage to SNpc in Stage III), to cognitive decline noted in advanced stages of the disease (due to damage to neocortex in Stage V, Figure 1).

Despite breakthroughs leading to better understanding of PD, the etiology of this disease and the mechanisms underlying neurodegeneration remain elusive. Currently, a variety of originating factors, including genetic predisposition, exposure to environmental toxins and traumatic brain injury are thought to induce PD related phenotypes through several pathological mechanisms including mitochondrial dysfunction, increased oxidative stress, altered proteolysis and inflammatory change.

New insight into the disease was made possible by the discovery of several genetic mutations which are associated with the development of PD. While most cases of PD (90%) are considered idiopathic, these genetic mutations can explain a small percentage (10%) of disease cases. A better understanding of genetically linked PD may also improve our understanding of idiopathic PD. PD associated genes may exert their effect through a variety of pathological mechanisms such as forming protein aggregates *(SNCA genes*), disrupting protein degradation (*Parkin and UCHL1*), protein misfolding (*DJ-1*), impairment of lysosomal function (*ATP13A2*) and mitochondrial dysfunction *(PINK1, LRRK2*).

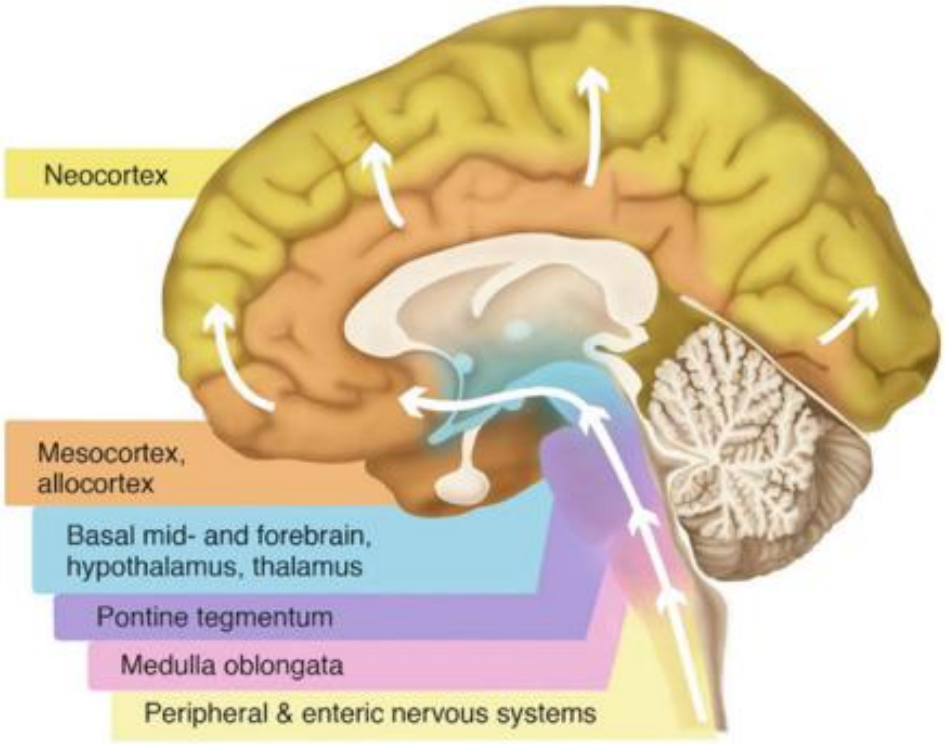

Figure 1: Progression of Parkinson disease.

The progression of Parkinson disease, according to the Braak Hypothesis. Lewy pathology follows a caudo-rostral path from the lower brain stem, through susceptible regions of the mid brain and forebrain, into the cerebral cortex (modified from Schneider and Obeso, 2014).

2.2 LRRK2: molecular structure, physiological role, and distribution

Mutations in the *leucine-rich repeat kinase-2* gene (*LRRK2/PARK8*) lead to autosomal dominant PD which is clinically indistinguishable from sporadic PD, suggesting similar underlying pathways (Paisan-Ruiz et al., 2004; Zimprich et al., 2004). The *leucine-rich repeat kinase-2* gene codes for an eponymous, large intracellular protein with multiple domains (Figure 2). LRRK2 is a member of the ROCO family of proteins and has two conserved domains that are characteristic of this protein family: a Ras of complex proteins (ROC) domain, and a C-terminal of ROC (COR) domain (Zimprich et al., 2004). The function of the COR domain is not known, however the ROC domain functions as a dimeric GTPase (Deng et al., 2008). In addition, several other conserved domains were identified in this protein, including a leucine-rich repeat (LRR), a kinase domain, a WD40 domain, and an ankyrin (ANK) repeat (Paisan-Ruiz et al., 2004; Zimprich et al., 2004). The leucine-rich repeat, WD40 domain, and ANK repeat are common features in many proteins and are thought to allow protein-protein interactions (Santperre and Ferrer, 2009), suggesting that LRRK2 may serve as a scaffold for the assembly of protein complexes (Tsika and Moore, 2013). The kinase domain of LRRK2 is a member of the super-family of serine and tyrosine kinases and has a similar structure to receptor-interacting protein (RIP) kinases, which are involved in activating cell death pathways in response to intracellular and extracellular signals (Meylan and Tschopp, 2005). The kinase activity of the protein is intramolecularly activated by the GTPase activity of the ROC domain (Guo et al., 2007; Ito et al., 2007). *In vivo* LRRK2 presents as a dimer, in which the ROC domain interactions with the LRR domain and the WD40 domain (Greggio et al., 2008). The numerous functional motifs found in LRRK2 suggest that this protein regulates a variety of cellular processes including mitochondrial function, signal transduction, cell death pathways, vesicle trafficking, neurite outgrowth, autophagy and cytoskeleton assembly (Santperre and Ferrer, 2009; Cookson et al., 2010; Berwick et al., 2011; Tsika and Moore, 2012).

In adult humans, LRRK2 mRNA and protein is expressed in several tissues including the brain, lungs, liver, kidney, spleen and in low levels in the heart (Paisan-Ruiz et al., 2004;

Zimprich et al 2004; Miklossy et al., 2006; Westerlund et al., 2008). Within the brain LRRK2 mRNA and protein expression is highest in the striatum, but is also found in the frontal cerebal cortex, hippocampus, cerebellum, locus coreulus and the substantia nigra (Galter et al., 2006; Higashi et al., 2007b; Westerlund et al., 2008; Vitte et al., 2010). Within the neuron, LRRK2 localizes in a variety of structures including the mitochondria, the endoplasmic reticulum, lysosomes and the cytoplasm (Biskup et al., 2006; Alegre-Abarratequi et al., 2009; Vitte et al., 2010). In addition to localizing in these subcellular structures in the cell body, LRRK2 is also found in dendrites and axonal processes (Higashi et al., 2007b). In the PD brain, overall neuronal expression of LRRK2 mRNA does not differ significantly from control brains (Sharma et al., 2011), however the LRRK2 protein has been shown to be a component of Lewy bodies in the brainstem, the substantia nigra and the locus coreulus (Higashi et al., 2007b; Vitte et al., 2010; Sharma et al., 2011), though results can differ depending on the antibody used. Despite no change in LRRK2 mRNA expression between control and PD cases in the frontal cortex, LRRK2 protein expression is enhanced in sporadic PD patients, suggesting post-transcriptional modification or a failure to clear proteins (Cho et al., 2013).

LRRK2 mRNA and protein expression is relatively abundant in almost all brain regions in the mouse brain including the striatum, cortex and the substantia nigra (Simon-Sanchez et al., 2006; Higashi et al., 2007a; Melrose et al., 2007; Giesert et al., 2013). In contrast, LRRK2 mRNA expression in the rat brain is more restricted. In adult rat brains, high expression has been noted in the medium spiny neurons of the striatum (Galter et al., 2006; Taymans et al., 2006; Westerlund et al., 2008), the pyramidal neurons of cerebral cortex (Taymans et al., 2006; Westerlund et al., 2008), the piriform cortex (Westerlund et al., 2008), the hippocampus (Taymans et al., 2006) and in the sensory dorsal root (Westerlund et al., 2008). Lower levels of LRRK2 mRNA have also been noted in the rat hypothalamus, olfactory bulb and substantia nigra (Taymans et al., 2006). In rats, temporal expression of LRRK2 in the striatum mirrors the postnatal development of dopamine innervations of the striatum which underscores the link of LRRK2 to dopaminergic neurons and the importance of LRRK2 malfunction in PD pathogenesis (Westerlund et al., 2008).

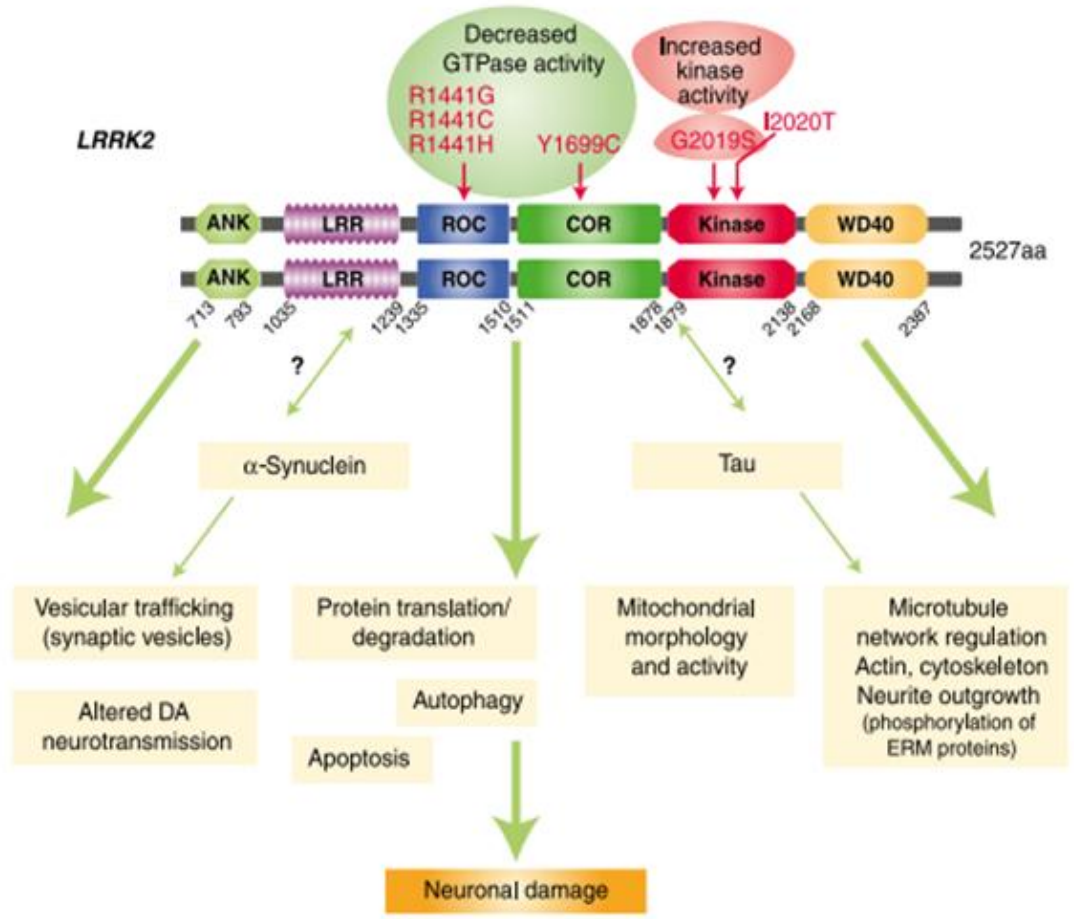

Figure 2: LRRK2 Structure.

LRRK2 is multi-domain protein with a catalytic core (ROC-COR-kinase) surrounded by protein-protein interaction domains (ANK, LRR and WD40). Most pathogenic mutations affect the GTPase and kinase activity of this protein. LRRK2 has been implicated in a variety of cellular roles including mitochondrial function, vesicular trafficking, neurotransmission, cell death pathways, cytoskeleton organization (modified from Tsika and Moore, 2012).

2.3 PD Related LRRK2 Mutations

Since the discovery of the link between *LRRK2* and Parkinson disease, six mutations have been identified in the *LRRK2* gene with several other mutations increasing PD risk (Zimprich et al., 2004; Berg et al., 2005; Di Fonzo et al., 2005; Goldwurm et al., 2005; Di Fonzo et al., 2006; Clark et al., 2006; Santpere and Ferrer, 2009; Zhang et al., 2009; Seki et al., 2011; Bozi et al., 2013; Anfossi et al., 2014; De Ross et al., 2014). Together these *LRRK2* mutations account for 13% of familial PD cases and 5% of sporadic cases (Berg et al., 2005; Santpere and Ferrer, 2009). These pathogenic mutations have been found in the kinase (G2019S, I2020T), ROC (R1441C/G/H), LRR (I1122V) and COR (Y1699C) domains (Santpere and Ferrer, 2009). Regardless of the domain of origin, many pathogenic mutations alter the kinase and GTPase activity of LRRK2 suggesting that these functions are particularly important in PD pathogenesis (Li et al., 2007; Deng et al., 2008; Anand and Braithwaite, 2009; Greggio, 2012; Biosa et al., 2013; Tsika and Moore, 2013; Ray et al., 2014).

The most common mutation, G2019S, is found in the kinase domain and increases the kinase activity of the LRRK2 protein by forcing the protein to remain in an active state (Berg et al., 2005; Funayama et al., 2005; Toft et al., 2005). When kinase capabilities of LRRK2 are genetically inactivated, cellular phenotypes including neuronal death and protein inclusions are greatly reduced, suggesting that kinase activity plays a crucial role in cell toxicity (Greggio et al., 2006; Smith et al., 2006; Iaccarino et al., 2007). The G2019S mutation may induce hyperphosporylation of tau, which in turn results in dendrite degeneration (Lin et al., 2010). The kinase domain has also been shown to phosphorylate sequences within the ROC domain, and therefore may regulate the GTPase activity of LRRK2 (Greggio et al., 2008; Pungaliya et al., 2010).

The second most common site of PD related *LRRK2* mutations is the R1441 “hotspot” amino acid codon where glycine, histidine and cysteine substitutions can occur. The R1441C/G/H mutations are in the ROC domain and affect the GTPase activity of the protein. The LRRK2 protein shows low intrinsic GTPase activity, however, this may be increased *in vivo* through binding with co-factors (Guo et al., 2007; West et al., 2007). Interestingly, mutations within the GTPase domain, including R1441G, increase kinase

activity through alteration of GTPase activity (West et al., 2007; Greggio et al., 2012; Tsika and Moore, 2013; Liao et al., 2014; Muda et al., 2014). Taken together, evidence suggests that the pathogenic effect of LRRK2 mutations depends on interplay between the GTPase and kinase activities of the protein. However, the intrinsic regulation which leads to LRRK2 toxicity remains unclear.

2.4 Genetic LRRK2 Animal Models

Modeling PD in animals can extend our understanding of etiology, pathogenesis and development of Parkinson disease. Currently, PD therapies are symptomatic and do not address the underlying pathogenic processes. A comprehensive animal model that recapitulates the full spectrum of the disease would allow the development of therapeutic strategies which specifically targeted the pathogenic process. *Drosophila LRRK2* models of Parkinson disease have recapitulated many features of PD including reduced dopamine content, neuronal loss, mitochondrial abnormalities, and decreased locomotor activity which can be ameliorated by L-DOPA (Imai et al., 2008; Liu et al., 2008; Ng et al., 2009; Venderova et al., 2009). In addition, *C.elegans* models of *LRRK2* mediated PD indicate age-dependent dopaminergic neurodegeneration, behavioural deficits and locomotor dysfunction (Yao et al., 2010). The success of these invertebrate models of Parkinson disease has prompted their validation in mammals. Several rodent models test the pathophysiology of *LRRK2* in Parkinson disease, as well as attempt to recapitulate cardinal features of the disease. Aberrant LRRK2 in Parkinson disease is thought to mediate neurotoxicity through a gain of function, perhaps due to an increase in kinase activity. Knock in and knock out models can provide support for this hypothesis by investigating the function of neuronal system under abnormal levels of LRRK2. Indeed, LRRK2 knockout mice display intact dopaminergic function and an absence of PD related phenotypes (Andres-Mateos et al., 2009; Tong et al., 2010; Hinkle et al., 2012), suggesting that an increase in the activity of LRRK2 is required for disease pathogenesis. Recently transgenic mouse models have been developed that carry missense PD related *LRRK2* mutations. These models may provide unique insight into the mechanisms through which familial *LRRK2* mutations cause PD pathogenesis. Li and colleagues describe a $LRRK2^{R1441G}$ BAC transgenic mouse line that recapitulates human PD

phenotypes (Li et al., 2009). These mice showed L-DOPA responsive, age dependent motor deficits starting at 6 months of age and progressively worsening by 12 months of age (Li et al., 2009). While these animals did not show dopaminergic neuron degeneration in the SNpc or aggregation of α-synuclein, dopamine release was impaired in these animals and axonal dystrophy reminiscent of PD was noted in the striatum (Li et al., 2009). Following studies with *LRRK2*^{R1441G} mice have largely failed to reproduce the motor dysfunction originally noted, however, mild Parkinsonism, gastrointestinal dysfunction , a common non-motor feature of PD, and impaired dopaminergic transmission have since been reported in some transgenic models (Bichler et al., 2013; Dranka et al., 2013). *LRRK2*^{G2019S} rodents have shown similarly mixed results with some groups reporting PD related phenotypes, including degeneration of dopaminergic neurons, hypoactivity, and impaired adult neurogenesis (Winner et al., 2011; Chen et al., 2012), while others fail to recapitulate key features of the Parkinsonian process including neurodegeneration (Zhou et al., 2011; Chou et al., 2014) and impaired locomotor ability (Ramonet et al., 2011). Overall these transgenic rodent models fail to display substantial PD pathology. One explanation for these results may be that multiple factors, such as interactions with other genes or environmental stressors are required to inhibit compensatory mechanisms and facilitate the degenerative process.

2.5 Mechanisms of LRRK2-mediated neurodegeneration

Although the underlying mechanisms through which LRRK2 mediates PD pathogenesis are still unclear, the molecular structure and distribution of LRRK2 can provide some insight into cellular pathways which are compromised in familial mutations. The presence of multiple protein-protein interaction domains in LRRK2 (ANK, LRR, WD40) suggest that it plays a role in maintaining the integrity of the cytoskeleton. In PD, degeneration of dopaminergic neurons in the SNpc is preceded by a loss of dopaminergic axonal projections from the substantia nigra into the striatum. Recent studies suggest that LRRK2 may play a role in the maintaining neuronal process integrity. Overexpression of *LRRK2* mutants results in a reduction in neurite length, axonal arborization, and the formation of tau-positive inclusions, which eventually lead to neuronal death (MacLeod

et al., 2006; Parisiadou et al., 2009; Ramonet et al., 2011; Sepulveda et al., 2013). Conversely, suppression of *LRRK2* results in the opposite phenotype of increased neuron process length, suggesting that LRRK2's normal role in maintaining neuronal process integrity is disrupted by familial mutations (MacLeod et al., 2006; Parisiadou et al., 2009). While it is still unclear how LRRK2 alters neurite morphology, the protein has been shown to interact with ezrin/radixin/moesin (ERM) family of proteins and Rac1, which are implicated in cell motility and actin skeletal dynamics (Parisiadou et al., 2009; Chan et al., 2011). In addition, the ROC domain in LRRK2 interacts with β-tubulin and this interaction is disrupted by the R1441G mutation, suggesting a role for LRRK2 in microtubule stability (Gandhi et al., 2008; Gillardon et al., 2009; Law et al., 2014). Neurite remodeling in *LRRK2* mediated PD might be a result of autophagic imbalance. Plowey et al. (2008) found that neurite retraction, in G2019S *LRRK2* expressing neuroblastoma cells, was significantly reduced when proteins necessary for autophagic induction were suppressed. Impaired autophagic imbalance, specifically the accumulation of large autophagic vacuoles with incompletely degraded materials, have since been reported by various groups in both cells cultures (Alegre-Abarratequi et al., 2009; Manzoni et al., 2013; Schapansky et al., 2014) and animal models (Ramonet et al., 2011; Saha et al., 2014). The role of LRRK2 in autophagy may be of particular importance as disrupted autophagy has been known to induce neuronal death (Komatsu et al., 2006). Another mechanism through which LRRK2 is proposed to mediate neurodegeneration is through an increase in oxidative stress caused by mitochondrial dysfunction. The localization of LRRK2 to the outer mitochondrial membrane supports this hypothesis (Biskup et al., 2006). Wildtype LRRK2 seems to offer protection against agents that cause mitochondrial dysfunction including Rotenone, Paraquat, hydrogen peroxide and 6-OHDA (Ng et al., 2009; Saha et al., 2009; Nguyen et al., 2010; Pereira et al., 2014). Conversely, familial mutations in *LRRK2* do not offer protection against these agents and are associated with an increased level of ROS and mitochondrial dysfunction (Iaccarino et al., 2007; Ng et al., 2009; Saha et al., 2009; Heo et al., 2010; Nguyen et al., 2010; Pereira et al., 2014). The increased vulnerability of *LRRK2* mutants to oxidative stress may be caused by the interaction of mutated LRRK2 with dynamin like protein 1 (DLP1) which is a regulator of mitochondrial fission (Niu et al., 2012; Wang et al., 2012). These

results suggest that LRRK2's normal protective role against oxidative stress is compromised with familial mutations, thus providing a mechanism through which these mutations induce PD. While these studies have increased our understanding of cellular pathways implicated in LRRK2 mediated neurodegeneration, it is important to note that LRRK2 is a complex protein with several physiological functions and that PD phenotypes are likely a combination of dysfunction across cellular processes.

2.6 Environmental Toxins and PD

In addition to genetic causes, the development of Parkinson disease has been linked to exposure to environmental toxins, particularly agrochemicals that possess neurotoxicity (Allen and Levy, 2013). In 1983, a small group of young individuals presented with PD following 1-methly-4-phenyl-1,2,3,6-tetrahydropyridine (MPTP) intoxication (Langston et al., 1983). The discovery of toxin triggered parkinsonism prompted investigation into the association between the disease and environmental contaminants with several studies showing an increased risk for PD following pesticide exposure (Brown et al., 2006; Tanner et al., 2011; Liew et al., 2014). One of the many agrochemicals implicated in PD pathogenesis is Paraquat. Paraquat, or *N,N'*-dimethyl-4-4'-bipyridinium dichloride, is a widely used herbicide and pre-harvest desiccant. Paraquat's chemical structure resembles that of MPP^+ (1-methyl-4-phenylpyridium), the active metabolite of the neurotoxin MPTP. This chemical homology has prompted several studies to explore the causative connection between Paraquat exposure and Parkinson disease. Epidemiological studies investigating a correlation between Paraquat exposure and PD have yielded inconclusive results (Costello et al., 2009, Firestone et al., 2005, Pezzoli and Cereda, 2013, Tanner et al., 2011), perhaps due in part to the challenges in exposure assessment. However, human studies investigating Paraquat exposure in combination with other risk factors (such as exposure to chemical agents and traumatic brain injury) have demonstrated an increased PD risk (Brown et al., 2006; Peng et al., 2007; Costello et al., 2009; Tanner et al., 2011; Lee et al., 2012). In addition, Paraquat induced PD phenotypes such as dopaminergic neurodegeneration, substantia nigra reduction, decreased striatal tyrosine hydroxylase immunoreactivity and alpha-synuclein accumulation, have been

shown in animal studies (Chicchetti et al., 2005; Ossowska et al., 2006; Somayajulu-Nitu et al., 2009; Kumar et al., 2010; Singhal et al; 2011).

In plants, Paraquat interacts with photosystem 1 to generate reactive oxygen species (ROS). This results in increased toxicity due to excess ROS as well as inhibition of photosynthesis and CO_2 fixation. In rodents, Paraquat is able to cross the blood-brain barrier (BBB) through a carrier-mediated mechanism involving the neutral amino acid transporter (Shimizu et al., 2001). Recently, epidemiological studies have shown an increased risk for Paraquat induced PD in patients with genetic variants in the dopamine transporter (DAT), suggesting a role for DAT in Paraquat toxicity (Ritz et al., 2009). Paraquat in its native state is a divalent cation, PQ^{2+}, however it can be reduced by NADPH oxidase to the monovalent cation, PQ^{+}. PQ^{+} is a DAT substrate and can accumulate in dopaminergic neurons leading to increased oxidative stress and cytotoxicity (Rappold et al., 2011). In addition, PQ^{+} is a substrate for the organic cation transporter 3 (Oct3) which is expressed in non-DA cells in the substantia nigra (Rappold et al., 2011). Within the neuron, Paraquat's exact mechanism of action is poorly understood. However, Paraquat's toxicity is thought to be the result of excess generation of reactive oxygen species. Paraquat can be continuously oxidized and reduced (a process known as redox cycling) to produce superoxide molecules. Acute Paraquat exposure has been linked to excess production of intracellular ROS leading to cell apoptosis (Peng et al., 2004). Paraquat interacts with complex I and III of the electron transport chain resulting in an increase in H_2O_2 production (Drechsel and Patel, 2009). In addition, Paraquat may induce dopaminergic neuronal death through activation of the JNK pathway (Peng et al., 2004), and inhibition of autophagy (Wills et al., 2012).

2.7 Multiple Hit Hypothesis

Despite extensive research, the etiology of Parkinson disease remains unknown. Due to the relatively low incidence of familial PD (5-10%), it seems unlikely that a genetic mutation is sufficient to explain disease pathogenesis. Conversely, researchers have yet to discover a single shared insult in PD patients as epidemiological studies often report conflicting information. Taken together, this suggests that PD originates not from a singular cause, but from multiple causes working synergistically to induce disease

phenotypes. The 'multiple hit' hypothesis suggests that multiple risk factors interact to induce the degenerative process seen in Parkinson disease (Sulzer, 2007). A variety of factors have been shown to increase PD risk including aging (Driver et al., 2009; Collier et al., 2011), genetic mutations (Ross et al., 2008; Alcalay et al., 2010; Bonifati, 2010; Kim et al., 2010; Pan et al., 2012), exposure to environmental toxins (Baldereschi et al., 2003; Phillipson, 2014) and trauma to the brain (Hubble et al., 1993; Doder et al., 1999; Maher et al., 2002; Lee et al., 2012). In addition, several environmental factors such as smoking, alcohol consumption, caffeine consumption, and exercise seem to have a protective effect on PD risk (Saaksjarvi et al., 2014; Van der Mark et al., 2014; Zhang et al., 2014), which suggests that environment does play an important role in the development of this disease. The primary insult is proposed to result in cellular stress, while secondary insults result in the loss of protective pathways thus inducing neuronal death (Sulzer, 2007). Recently, several studies have provided supported for this hypothesis. In rodent models of toxin-induced PD, multiple toxins working in conjunction were shown to enhance PD neuropathology, including nigrostriatal dopaminergic cell loss and reduced striatal dopamine content (Thiruchelvam et al., 2003; Peng et al., 2007; Kumar et al., 2010). This is further supported by epidemiological studies which show an increased PD risk in individuals exposed to multiple agrochemicals (Tanner et al., 2011). Similarly, gene-environmental interactions have been shown to play an important role in the development of PD. Peng et al. (2010) showed that mice expressing the A53T familial mutant form of human α-synuclein showed increased susceptibility to neonatal iron feeding and Paraquat exposure. Nuber et al (2014) found that Paraquat exposure synergistically induced dopaminergic cell degeneration in mice overexpressing familial PD linked mutant α-synuclein. In addition, exposure to neurotoxins, maneb and Paraquat, alters regulation of adult neurogenesis in transgenic mice carrying the *SNCA* and $LRRK2^{G2019S}$ familial mutations (Desplats, 2012). In an epidemiological study, Ritz et al. (2009) found that individuals with dopamine transporter genetic variations showed an increased risk for PD following exposure to maneb or Paraquat. The combination of injury and exposure to environmental toxins has also been shown to increased PD risk. Hutson et al. (2011) showed that traumatic brain injury in adult rats increased vulnerability to Paraquat and caused degeneration of

dopaminergic SNpc neurons. This was later supported by an epidemiological study which noted increased incidence of PD in patients with traumatic brain injuries that had previously been exposed to Paraquat (Lee et al., 2012). These studies suggest that aetiology of Parkinson disease is a multifactorial. Animal models which explore the synergistic effect of combined PD risk factors can play an important role in furthering understanding of disease etiology.

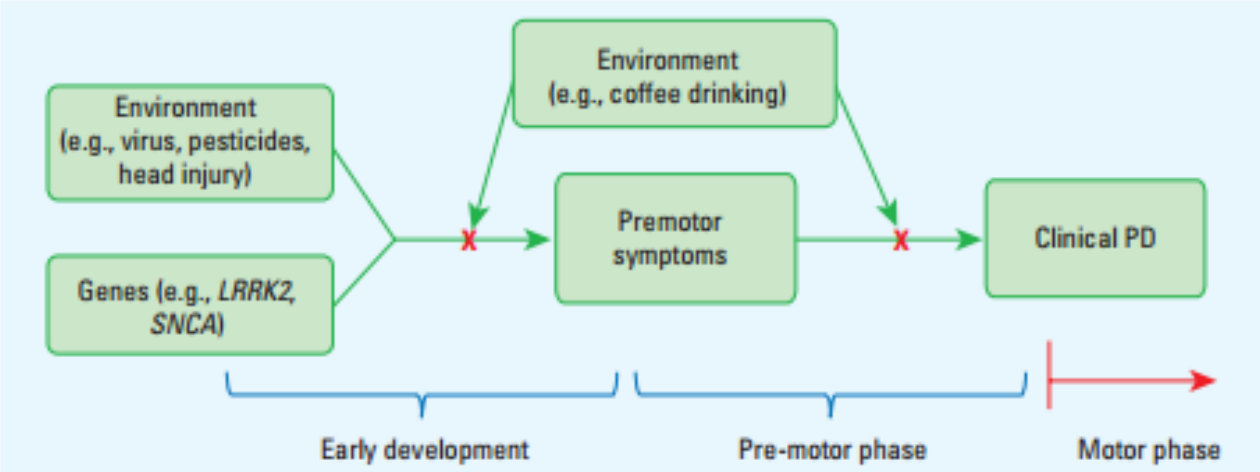

Figure 3: Multiple factors affect PD.

A proposed mechanism of multiple factors working in conjunction to induce Parkinson disease. Genetic predisposition for the disease can prime neurons for additional stress caused by environmental factors such as exposure to toxins or traumatic brain injury, which then leads to neurodegeneration. Protective environmental factors can reduce the likelihood of developing disease phenotypes. Adopted from Chen et al., 2013.

Chapter 3

3 Research Purpose and Hypotheses

The purpose of this study was to investigate the combined effect of a genetic predisposition and exposure to environmental toxins in the development of Parkinson disease. Transgenic rats expressing the human *LRRK2*^{R1441G} mutation were tested for motor and cognitive deficits, reminiscent of PD, in order to determine if a genetic mutation alone was sufficient to induce disease pathology. These rats were then exposed to the neurotoxin, Paraquat in order to test increased susceptibility of transgenic rats to environmental toxins. We hypothesized that *LRRK2*^{R1441G} rats show PD phenotypes by 12 months of age and that these rats will have an enhanced susceptibility to Paraquat.

Chapter 4

4 Materials and Methods

4.1 Study 1: Assessing PD-related phenotypes in *LRRK2*^{R1441G} transgenic rats

4.1.1 Animals

A commercially available breeding pair of Sprague Dawley rats expressing the R1441G mutation on the human gene *LRRK2* was obtained from Taconic (Line #10677). The original model was created by Dr. Chenjian Li through pronuclear injection of the human *LRRK2*^{R1441G} gene into Sprague Dawley zygotes. The line was maintained through in house breeding of hemizygous x wildtype breeding pairs. More information about the transgenic rat line used in this document can be found at http://www.taconic.com/10681. Rats were weaned at 3 weeks of age and genotyped to detect human *LRRK2.* Transgenic animals were housed with wildtype littermates in a 12 h light-dark cycle with food and water provided ad libitum. 17 wildtype and 24 *LRRK2*^{R1441G} transgenic rats underwent a battery of behavioral tests. Animals underwent behavioral tests at 3 months, 6 months, 9 months and 12 months of age. All animals were tested on each behavioural test described below at each of the four time points. All procedures were in accordance with the ethical guidelines of the Canadian Council on Animal Care (CCAC) and approved by the University of Western Ontario Animal Use Subcommittee.

4.1.2 Genotyping

Before weaning, all rats were genotyped by polymerase chain reaction (PCR) using tissue obtained from ear-punching. Genotyping was performed using an assay kit from Taconic according to their specifications. The PCR reaction combined 5 µL of genomic DNA (2 ng/µL), 2.5 µL of PCR Buffer (5 mM), 1 µL of $MgCl_2$ (2.5 mM), 0.5 µL of deoxynucleotide mixture (0.2 mM), 0.5 µL of hpark8-F primer (0.5µM), 0.5 µL of hpark8-R primer (0.5µM) and 0.25 µL of HotStarTaq DNA Polymerase (0.05U/µL). The thermocycler protocol involved 1 cycle (15 min) at 95ºC, combined 35 cycles with 45 s at 94ºC, 1 min at 65ºC, and 1 min at 72ºC, and 1 cycle at 72ºC (5 min). The primer sequence for the hpark8-F primer is GAT AGG CGG CTT TCA TTT TTC C and for the

hpark8-R primer is ACT CAG GCC CCA AAA ACG AG. Primers were generated in house at the University of Western Ontario.

4.1.3 Behavioral Testing

4.1.3.1 Vibrissae-evoked forelimb placing

The forelimb placing test was performed as previously described and used as a measure of movement initiation abilities (Schallert et al. 2002, Woodlee et al., 2005), a common deficit observed in PD patients. Briefly, the experimenter holds the animal aloft by its torso and brushes its vibrissae against the edge of the testing surface. This elicits a forelimb placing response from the limb on the same side. Placing is quantified as the percentage of correct responses or 'hits' elicited out of fifteen trials. Trials in which the animal struggles or resists the experimenter's grip are discounted. Animals were all trained on this task prior to testing in order to ensure acclimation to the experimenter as well as reduction in struggling behaviors.

4.1.3.2 Adjusting steps

The adjusting steps task has been extensively used to measure postural stability in rats (Olsson et al., 1995, Chang et al., 1999, Fleming et al., 2009). The experimenter holds the animal by its torso such that its hindlimbs are lifted above the testing surface. One forelimb is then restrained so that the animal's weight is entirely supported by the remaining free forelimb, which is in contact with the testing surface. The experimenter then moves the animal laterally across a testing surface with a distance of 70 cm. In order to compensate for the movement of the body, the animal should make adjusting steps with the weight-bearing forelimb. The average number of steps each animal makes over five trials is recorded and used for analysis. Animals with nigrostriatal degeneration will drag their forelimb instead of making the appropriate adjusting steps (Fleming et al., 2012).

4.1.3.3 Footprint Analysis

Footprint analysis was performed in order to assess stepping patterns and abnormal gait (Li et al., 2010). The rat's paws were dipped in non-toxic paint and the rat was placed on

a runway 110 cm long, 10 cm wide and with 25 cm high side walls. The runway led to the rat's homecage and rats were thus motivated to traverse the gangway. The floor of the runway was lined with ordinary paper and the footprints marked on the paper were analyzed. The distance between forepaws and the left and right stride were recorded.

4.1.3.4 Open Field Test

The open field test was used to measure general locomotor activity in wildtype and transgenic rats. Each animal was placed in a square activity box (Med Associates Activity Monitor, St. Albans, VT, USA) for 30 minutes per day, for two days. After each animal finished testing, the activity boxes were cleaned with 70% ethanol to eliminate any odors which may bias the next animal. Using the MedAssociates Activity Monitor software, we analyzed the distance traveled and the number of rearing movements during the testing interval. Exploratory rearing was used as an indirect measure of paucity of movement, as previously shown (Landers et al., 2014).

4.1.3.5 Acoustic Startle Response and Sensory Gating

The acoustic startle response of these animals was tested using a protocol similar to those previously described (Typlt et al., 2013). Startle testing was conducted in sound attenuated startle boxes from Med Associates (MED ASR PRO1, St Albans, VT, USA). Animals were placed in holders mounted on a movement sensitive platform within the startle box. A transducer converted the vertical movement of the platform, induced by the animal's startle response, into a voltage signal. The maximum amplitude of the signal was measured using Med Associates software (Startle Reflex Version 6, Med Associates, St Albanks, VT, USA). On day 1, animals were acclimated to the startle box and background noise (65 dB white noise) for 5 minutes in the morning and again for 5 minutes several hours later. On day 2, animals underwent an input-output (IO) test to determine the appropriate gain setting for each animal. The IO function has an initial stimulation at 65 dB (20 ms duration) and increased in 5 dB intervals to 120 dB. On day 3, animals were tested in two blocks for short term habituation and prepulse inhibition respectively. Block 1 assessed habituation by presenting 30 trials of the startle pulse (105 dB white noise, 20 ms duration and 15 ms intertribal interval). Block 2 assessed prepulse inhibition. In Block 2, there were seven different trial conditions (10 trials per condition)

for a total of 70 trials. The trials presented the startle pulse alone, a low prepulse of 75 dB (4 ms duration) before the startle pulse, and a high prepulse of 85 dB (4 ms duration) before the startle pulse. The presentation of the prepulse and the startling pulse was separated by three different interstimulus intervals (ISIs): 10 ms, 30 ms or 100 ms. The trials were presented in pseudorandomized order. Animals were tested on both habituation and prepulse inhibition as both responses are disrupted in PD patients (Matsumoto et al., 1992; Zoetmulder et al., 2014).

4.1.3.6 Morris Water Maze

Both wildtype and transgenic animals underwent two versions of the Morris water maze task to assess learning and memory, as previously described (Myoshi et al., 2002). This task was conducted in a round tank, 146 cm in diameter and 58 cm deep, filled with water. The water was colored with non-toxic blue paint to ensure opaqueness. Throughout testing, the water temperature was monitored and maintained at 21°C. The tank was divided into four equally sized quadrants and a circular acrylic escape platform was placed in one of the quadrants. The escape platform was submerged in water by 2 cm so that it was not visible to the animals. A camera mounted above the tank recorded the movement of the animals in each trial. The Any-maze Behavior Tracking Software (Stoelting Co., Wood Dale, IL, USA) was used to record the latency to reach the escape platform and the time spent in the target quadrant.

All animals were first tested on the cued version of the water maze task. This consisted of two training days with four trials on each day. In each trial, the animals were placed in the water facing the tank wall and had to locate the escape platform, which was cued by a yellow ball attached to the platform and protruding from the water. The trial was completed when the animal either found the escape platform or 90 s had passed. If the animal was unable to located the platform in 90 s, it was gently led to the platform. Animals were allowed to remain on the escape platform for 15 s before being removed and dried before the next trial. The initial position of the animal was the vertices of one of the four quadrants and was different for each trial. The initial position was assigned randomly and counterbalanced for the genotypes. The platform position was also changed between each trial and was randomly assigned and counterbalanced.

The animals were also tested on the spatial reference version of the water maze as previous described (Miyoshi et al., 2002). This consisted of four training days with four trials on each day. The experimental procedure was similar to the previous one, except that the location of the platform was no longer cued. Instead, animals could utilize external visual cues on the walls surrounding the tank to locate the platform. In addition, the platform position was kept constant between trials and days. The four trials of the first of the four training days were used as an indicator of spatial working memory.
On day 7, experimenters ran a 90 s probe trial without the platform. During this trial, the time spent in the target quadrant was recorded for each animal.

4.2 Study 2: Testing Paraquat Vulnerability in aged *LRRK2*^{R1441G} transgenic rats

4.2.1 Vulnerability to Paraquat

In study 2, all animals were exposed to an acute sub-toxic Paraquat regimen, as previously described, in order to assess vulnerability to toxins (Hutson et al., 2011). Animals were separated into four groups: wildtype-saline (n=8), wildtype-Paraquat (n=8), transgenic-saline (n=10), and transgenic-Paraquat (n=11). Animals received two IP injections of Paraquat (10 mg/kg dissolved in 0.9% saline) or saline, with three days in between injections. At the time of testing, animals were 14-16 months old. The toxin dose used in this study was ¼ of that previously shown to cause dopaminergic cell death in the substantia nigra in adult rats (Cicchetti et al., 2005). All animals underwent the open field test immediately after receiving injections and 24 hours after injections. As previously mentioned, MedAssociates Activity Monitor software was used to analyze the number of rearing movements during a 30 minute testing interval.

4.2.2 q-RT PCR

Some transgenic rats were perfused with saline and samples for various brain regions (cortex, substantia nigra, hippocampus), as well as liver and kidney were obtained and frozen on ice. RNA was isolated using QIAzol Lysis Reagent (Qiagen, Germantown, MD, CA) according to the manufacturer's instructions. cDNA was synthesized using Life Technologies high-capacity cDNA Reverse Transcription Kit (Life Technologies, Grand

Island, NY, USA). Real time PCR assays were performed in triplicate on a 384 well plate. The level of human *LRRK2* mRNA was detected using TaqMan probe Hs00411197_ml specific for human LRRK2 (Life Technologies, Grand Island, NY, USA). The housekeeping gene GAPDH was detected using Rn01775763 (Life Technologies, Grand Island, NY, USA) and was used as a reference gene.

4.2.3 Statistical Analysis

Mean values ± standard error are reported. Outliers, defined as data points three standard deviations from the mean, were identified and removed from the data set. Comparisons of genotype and treatment groups were performed using repeated measures ANOVA. IBM SPSS Statistics 2.0 software was used for all statistical analyses. Results were considered statistically significant at a p value of 0.05.

Chapter 5

5 Results

5.1 Study 1: Assessing PD-related phenotypes in *LRRK2*^{R1441G} transgenic rats

All animals were weighed before behavioral testing, at each age point. All rats significantly increased their weight over time [ANOVA $F(2,75)=378,90$, $p<0.001$, Greenhouse-Geisser correction], however there was no significant difference in weight between transgenic *LRRK2*^{R1441G} rats and their wildtype littermates [ANOVA $F(2,75)=0.63$, $p=0.52$, Greenhouse-Geisser correction; Figure 4].

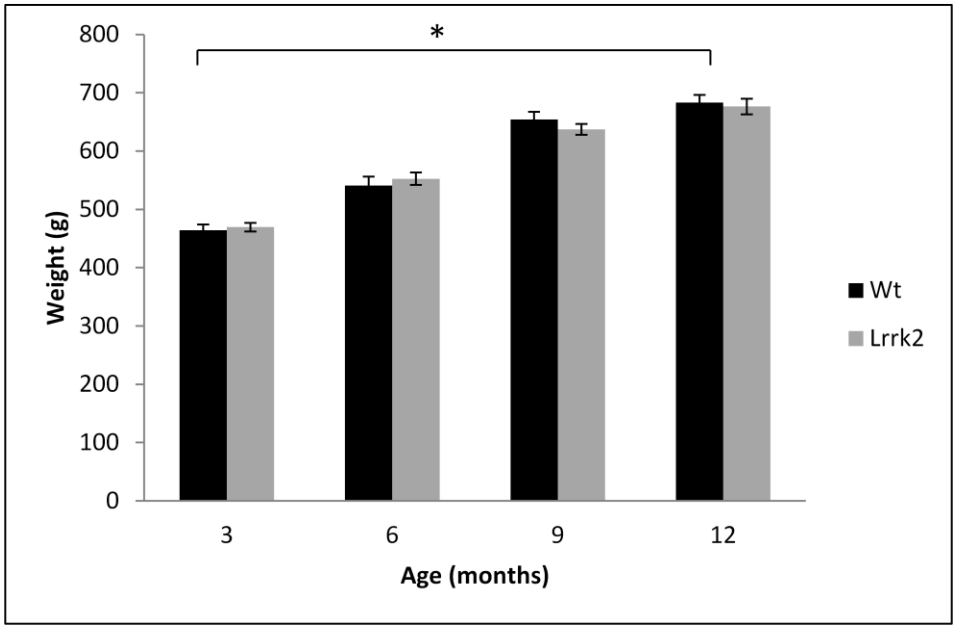

Figure 4: Rat Weight.

All rats were weighed before behavioral testing. There was no significant difference in weight between wildtype and transgenic *LRRK2*^{R1441G} rats at 3 (*LRRK2*^{R1441G}: M=469.46, SEM=7.58; WT: M=464.35, SEM=9.84), 6 (*LRRK2*^{R1441G}: M=552.46, SEM=10.55; WT: M=653.10, SEM=13.17), 9 (*LRRK2*^{R1441G}: M=636.99, SEM=9.24; WT:M=653.96, SEM=13.17), and 12 (*LRRK2*^{R1441G}: M=676.46, SEM=13.37; WT: M=683.17,

SEM=12.98) months of age [ANOVA $F(2,75)=0.63$, $p=0.52$, Greenhouse-Geisser correction].

5.1.1 Motor Tests

5.1.1.1 Vibrissae-evoked forelimb placing

In order to assess movement initiation abilities, vibrissae-evoked forelimb placing responses were measured in transgenic *LRRK2*^{R1441G} rats and their wildtype littermates at 3, 6, 9 and 12 months of age. While a significant main effect of age was noted in forelimb placing responses [ANOVA $F(2,85)=8.14$, $p<0.05$, Huynh-Feldt correction], no genotype and age interaction was noted [ANOVA $F(2,85)=0.37$, $p=0.71$, Huynh-Feldt correction]. Therefore, transgenic *LRRK2*^{R1441G} did not significantly differ from wildtype rats in vibrissae-evoked forelimb placing, suggesting intact movement initiation abilities (Figure 5).

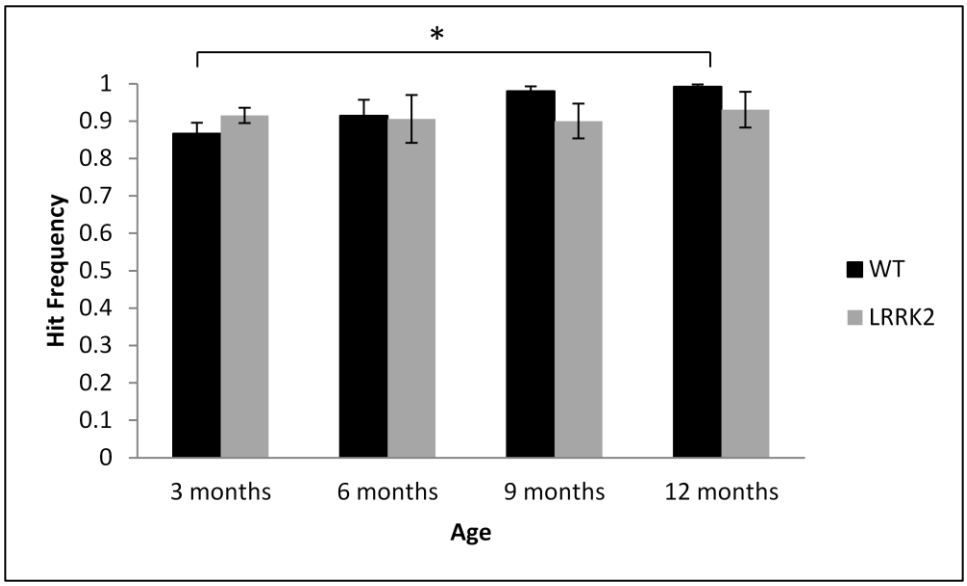

Figure 5: Vibrissae Evoked Forelimb Placing.

Vibrissae evoked forelimb placing was measured in transgenic *LRRK2*^{R1441G} rats and wildtype littermates. There was no significant difference in forelimb placing between wildtype and transgenic *LRRK2*^{R1441G} rats at 3 (*LRRK2*^{R1441G}: M=0.87, SEM=0.02; WT: M=0.87, SEM=0.02), 6 (*LRRK2*^{R1441G}: M=0.91, SEM=0.06; WT: M=0.91, SEM=0.04), 9 (*LRRK2*^{R1441G}: M=0.90, SEM=0.05; WT:M=0.98, SEM=0.01), and 12 (*LRRK2*^{R1441G}:

M=0.93, SEM=0.05; WT: M=0.99, SEM=0.01) months of age [ANOVA $F(2,85)=0.37$, $p=0.71$, Huynh-Feldt correction].

5.1.1.2 Adjusting steps

Postural stability in *LRRK2*^{R1441G} rats was measured using the adjusting steps task. While a small but significant main effect of age was noted in the number of adjusting steps made [ANOVA $F(3,102)=3.40$, $p<0.05$, Huynh-Feldt correction], no genotype and age interaction was noted [ANOVA $F(3,102)=1.06$, $p=0.37$, Huynh-Feldt correction]. Therefore, transgenic *LRRK2*^{R1441G} rats did not significantly differ from wildtype rats in the adjusting steps task, suggesting normal postural stability (Figure 6).

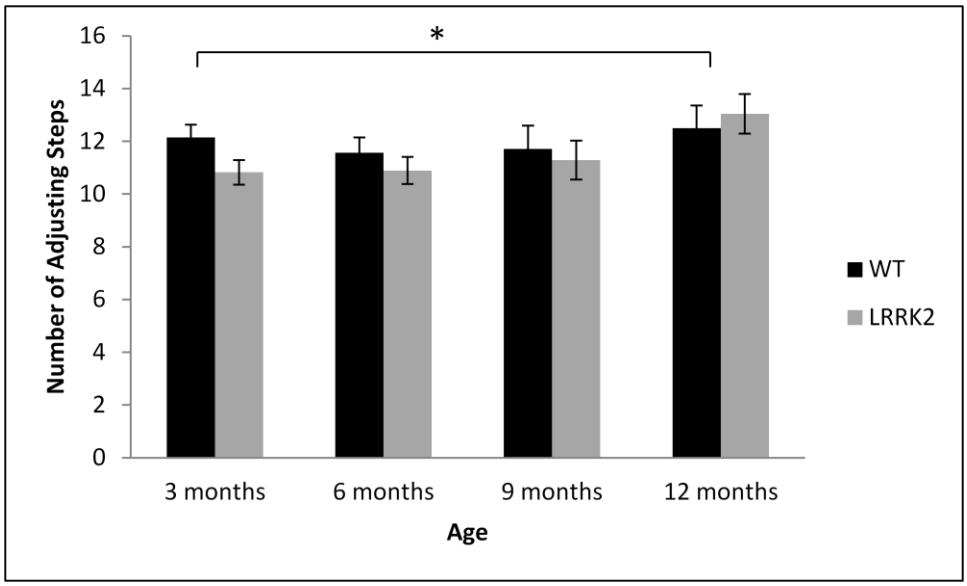

Figure 6: Adjusting Steps Task.

Performance on the adjusting steps task was measured in all animals. No significant difference in adjusting steps was noted between transgenic *LRRK2*^{R1441G} rats and wildtype littermates at 3 (*LRRK2*^{R1441G}: M=10.82, SEM=0.47; WT: M=12.15, SEM=0.48), 6 (*LRRK2*^{R1441G}: M=10.89, SEM=0.51; WT: M=11.56, SEM=0.58), 9 (*LRRK2*^{R1441G}: M=11.28, SEM=0.73; WT:M=11.71, SEM=0.88), and 12 (*LRRK2*^{R1441G}: M=13.04, SEM=0.75; WT: M=12.50, SEM=0.85) months of age [ANOVA $F(2,85)=0.37$, $p=0.71$, Huynh-Feldt correction].

5.1.1.3 Footprint Analysis

Foot print analysis was conducted on all animals in order to assess gait patterns. A main effect of age was noted in stride length of animals [ANOVA $F(3,105)=37.36$, $p<0.05$, Huynh-Feldt correction]. Both right and left stride lengths were measured in all animals, however, no main effect of side was noted [ANOVA $F(1,39)=0.12$, $p=0.72$, Huynh-Feldt correction]. In addition, there was no interaction between age, side and genotype [ANOVA $F(3,117)=0.60$, $p=0.62$, Huynh-Feldt correction].Therefore *LRRK2*^{R1441G} rats showed normal gait patterns as compared to wildtype controls (Figure 7).

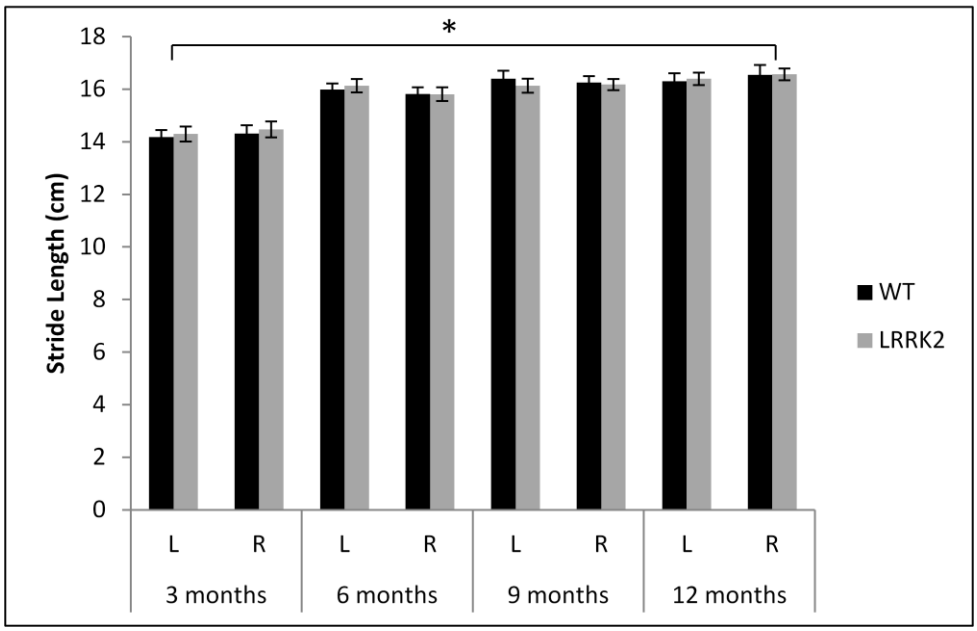

Figure 7: Stride Length.

Stride length was calculated on each side (L indicates left side and R indicates right side) in each animal and averaged within genotype. There was no significant difference in stride length in transgenic *LRRK2*^{R1441G} rats and wildtype littermates at 3 (*LRRK2*^{R1441G} Left M=14.30, SEM=0.29; *LRRK2*^{R1441G} Right M=14.47, SEM=0.30; WT Left M=14.18, SEM=0.27; WT Right M=14.31, SEM=0.31), 6 (*LRRK2*^{R1441G} Left M=16.13, SEM=0.25; *LRRK2*^{R1441G} Right M=15.81, SEM=0.26; WT Left M=15.99, SEM=0.23; WT Right M=15.82, SEM=0.26), 9 (*LRRK2*^{R1441G} Left M=16.13, SEM=0.26; *LRRK2*^{R1441G} Right M=16.18, SEM=0.22; WT Left M=16.40, SEM=0.30; WT Right M=16.25, SEM=0.24) and 12 (*LRRK2*^{R1441G} Left M=16.39, SEM=0.24; *LRRK2*^{R1441G} Right M=16.56,

SEM=0.22; WT Left M=16.30, SEM=0.31; WT Right M=16.55, SEM=0.37) months of age [ANOVA $F(3,117)=0.60$, $p=0.62$, Huynh-Feldt correction].

5.1.1.4 Open Field Test

Locomotor activity of transgenic *LRRK2*^{R1441G} rats and wildtype controls was assessed on the open field test. Animals were tested for two 30 minute sessions across two consecutive days. Data presented here is calculated across both sessions. There was no significant difference between transgenic and wildtype animals in the total distance travelled during the two sessions [ANOVA $F(3,102)=0.47$, $p=0.67$, Huynh-Feldt correction], although a main effect of age was noted [ANOVA $F(3,102)=29.71$, $p<0.001$, Huynh-Feldt correction; Figure 8]. Similarly, no significant difference in rearing behavior was noted between transgenic and wildtype rats [ANOVA $F(3,103)=0.79$, $p=0.49$, Huynh-Feldt correction], although a main effect of age was noted [ANOVA $F(3,102)=19.33$, $p<0.001$, Huynh-Feldt correction; Figure 9]. Finally, there was no difference in maximal velocity of transgenic *LRRK2*^{R1441G} rats and wildtype controls [ANOVA $F(3,117)=0.59$, $p=0.62$; Figure 10].

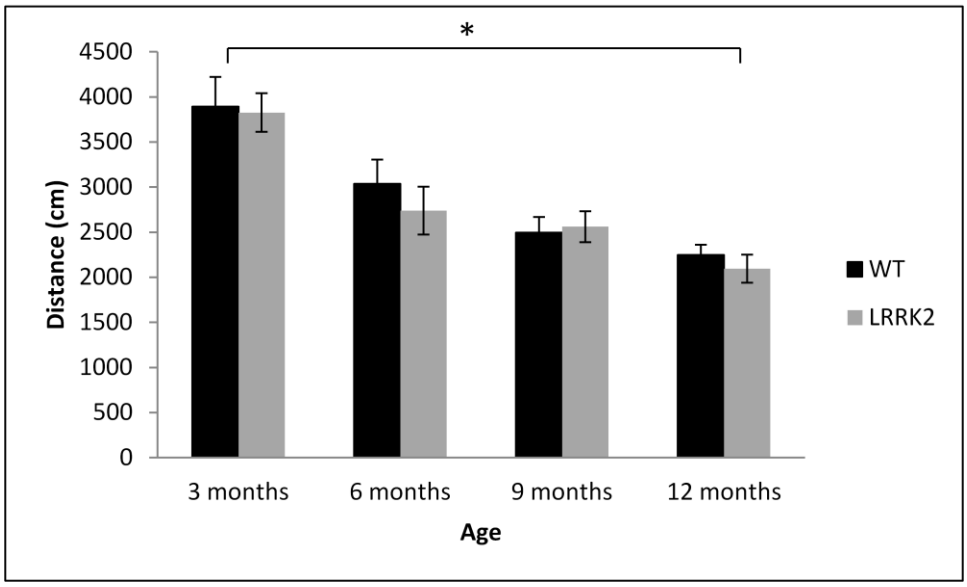

Figure 8: Total distance travelled in open field test.

Total distance travelled across testing sessions was calculated for all animals. No significant difference in total distance travelled was noted between transgenic *LRRK2*^{R1441G} rats and wildtype littermates at 3 (*LRRK2*^{R1441G}: M=3826.80, SEM=213.48; WT: M=3892.54, SEM=330.19), 6 (*LRRK2*^{R1441G}: M=2739.56, SEM=265.96; WT: M=3036.17, SEM=267.54), 9 (*LRRK2*^{R1441G}: M=2561.25, SEM=171.28; WT:M=2494.14, SEM=174.34), and 12 (*LRRK2*^{R1441G}: M=2094.07, SEM=156.20; WT: M=2248.38, SEM=110.60) months of age [ANOVA $F(3,102)=0.47$, $p=0.67$, Huynh-Feldt correction]. The distance travelled by all animals decreased as they aged [ANOVA $F(3,102)=29.71$, $p<0.001$, Huynh-Feldt correction].

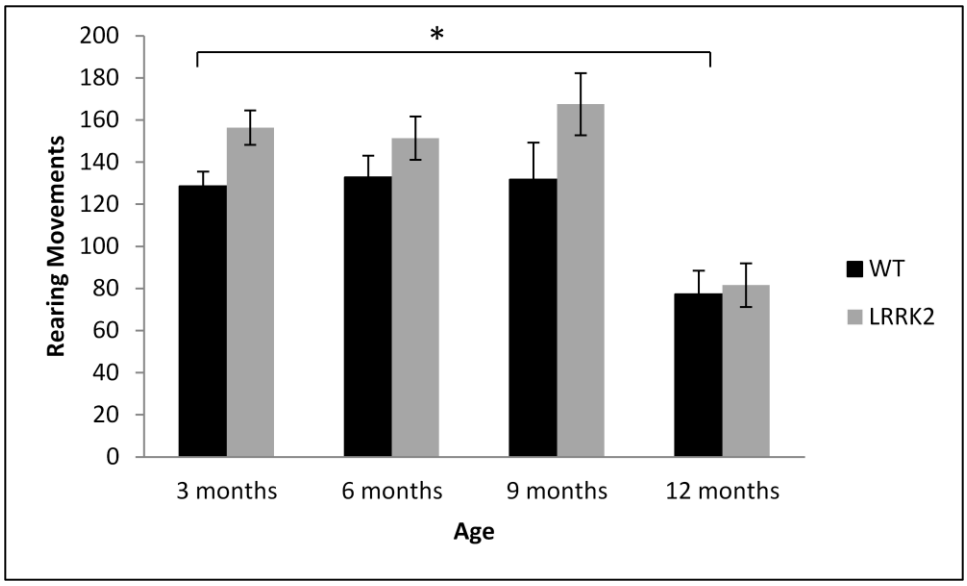

Figure 9: Rearing behavior in open field test.

Rearing movements made by all animals was summed across testing sessions. No significant difference in rearing movements was noted between transgenic *LRRK2*^{R1441G} rats and wildtype littermates at 3 (*LRRK2*^{R1441G}: M=156.38, SEM=8.14; WT: M=128.53, SEM=6.98), 6 (*LRRK2*^{R1441G}: M=151.38, SEM=10.30; WT: M=132.76, SEM=10.28), 9 (*LRRK2*^{R1441G}: M=167.50, SEM=14.72; WT:M=131.76, SEM=17.55), and 12 (*LRRK2*^{R1441G}: M=81.58, SEM=10.36; WT: M=77.29, SEM=11.21) months of age [ANOVA $F(3,103)=0.79$, $p=0.49$, Huynh-Feldt correction]. The total number of rearing movements decreased as rats aged [ANOVA $F(3,102)=19.33$, $p<0.001$, Huynh-Feldt correction].

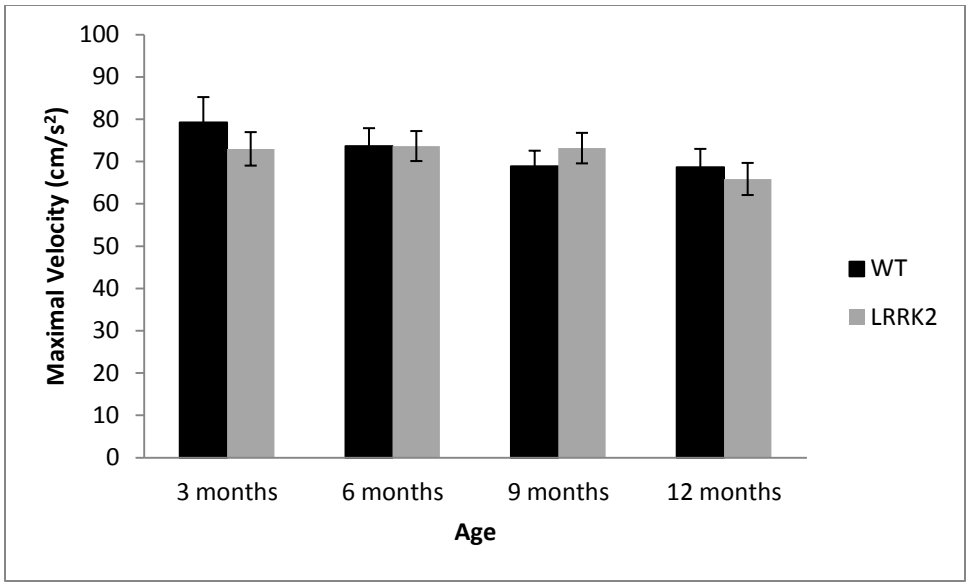

Figure 10: Maximal velocity in open field test.

Maximal velocity of transgenic and wildtype rats was calculated across testing sessions. No significant difference in maximal velocity was noted between transgenic *LRRK2*^{R1441G} rats and wildtype littermates at 3 (*LRRK2*^{R1441G}: M=72.99, SEM=3.96; WT: M=79.22, SEM=6.01), 6 (*LRRK2*^{R1441G}: M=73.65, SEM=3.54; WT: M=73.62, SEM=4.26), 9 (*LRRK2*^{R1441G}: M=73.17, SEM=3.61; WT:M=68.88, SEM=3.68), and 12 (*LRRK2*^{R1441G}: M=65.87, SEM=3.79; WT: M=68.63, SEM=4.36) months of age [ANOVA $F(3,117)=0.59$, $p=0.62$].

5.1.2 Cognitive Tests

5.1.2.1 Acoustic Startle Response and Sensory Gating

The acoustic startle response was measured in all rats in order to investigate sensory gating mechanisms, including habituation and prepulse inhibition. Baseline startle amplitude was calculated at the onset of sensory gating testing at each age point and was not significantly different between transgenic and wildtype rats [ANOVA $F(2,103)=0.32$, $p=0.79$, Huynh-Feldt correction; Figure 11]. Habituation scores were calculated by dividing the average of the last five startle responses by the maximum of the first three startle responses. Habituation scores of transgenic *LRRK2*^{R1441G} rats and wildtype littermates did not significantly differ [ANOVA $F(3,102)=0.33$, $p=0.78$, Huynh-Feldt

correction*;* Figure 12]. Habituation was also measured by examining the attenuation of startle response over time at each age point. At 3 months of age, a significant decrease in startle amplitude was noted [ANOVA $F(16,643)=3.29$, $p<0.001$, Huynh-Feldt correction], however there was no significant difference between transgenic and wildtype rats [ANOVA $F(16, 643)=0.68$, $p=0.82$, Huynh-Feldt correction; Figure 13]. Similarly habituation was observed in all animals at 6 [ANOVA $F(12,476)=2.85$, $p<0.001$, Huynh-Feldt correction; Figure 14], 9 [ANOVA $F(16,640)=1.91$, $p<0.05$, Huynh-Feldt correction; Figure 15] and 12 [ANOVA $F(16,637)=2.97$, $p<0.001$, Huynh-Feldt correction; Figure 16] months of age but no significant difference between the genotypes was observed [6 months ANOVA $F(12,476)=0.78$, $p=0.67$, Huynh-Feldt correction; 9 months ANOVA $F(16,640)=1.04$, $p=0.42$, Huynh-Feldt correction; 12 months ANOVA $F(16,637)=0.92$, $p=0.55$, Huynh-Feldt correction].

In addition, prepulse inhibition was measured in all rats using two different prepulse levels (75 dB and 85 dB) and three different interstimulus intervals (10 ms, 30 ms, 100 ms). At 3 months, a significant main effect of prepulse [ANOVA $F(1,39)=32.10$, $p<0.001$; Figure 17 and Figure 18] and ISI was noted [ANOVA $F(2,78)=10.28$, $p<0.001$], however there was no significant difference between transgenic and wildtype rats [ANOVA $F(2,78)=0.64$, $p=0.53$]. Therefore at 3 months of age, all rats displayed prepulse inhibition, with no significant difference between the two genotypes. Similarly, prepulse inhibition was noted at 6 [ANOVA $F(1,39)=61.53$, $p<0.001$, Huynh-Feldt correction; Figure 19 and Figure 20], 9 [ANOVA $F(1,39)=30.40$, $p<0.001$, Huynh-Feldt correction; Figure 21 and Figure 22], and 12 months of age [ANOVA $F(1,39)=29.83$, $p<0.001$, Huynh-Feldt correction; Figure 23 and Figure 24], however there was no difference in the extent of inhibition between transgenic $LRRK2^{R1441G}$ rats and wildtype controls [6 months ANOVA $F(2,61)=0.228$, $p=0.74$, Huynh-Feldt correction; 9 months ANOVA $F(2,78)=1.49$, $p=0.23$, Huynh-Feldt correction; 12 months ANOVA $F(2,78)=1.59$, $p=0.21$, Huynh-Feldt correction].

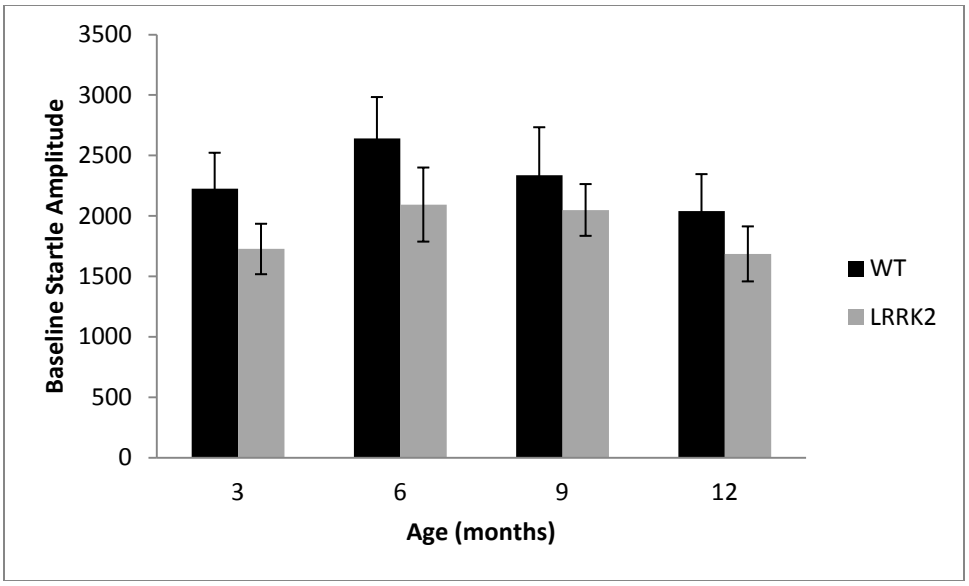

Figure 11: Baseline startle amplitude.

Baseline startle amplitude was measured by calculating the maximum startle response within the first three trials. Baseline startle amplitude did not differ between transgenic *LRRK2*^{R1441G} rats and wildtype littermates at 3 (*LRRK2*^{R1441G}: M=1726.38, SEM=208.64; WT: M=2224.03, SEM=298.55), 6 (*LRRK2*^{R1441G}: M=2093.78, SEM=306.49; WT: M=2641.25, SEM=342.10), 9 (*LRRK2*^{R1441G}: M=2049.21, SEM=214.26; WT:M=2337.33, SEM=396.26), and 12 (*LRRK2*^{R1441G}: M=1685.81, SEM=227.55; WT: M=2040.29, SEM=305.36) months of age [ANOVA $F(3,103)=0.32$, $p=0.79$].

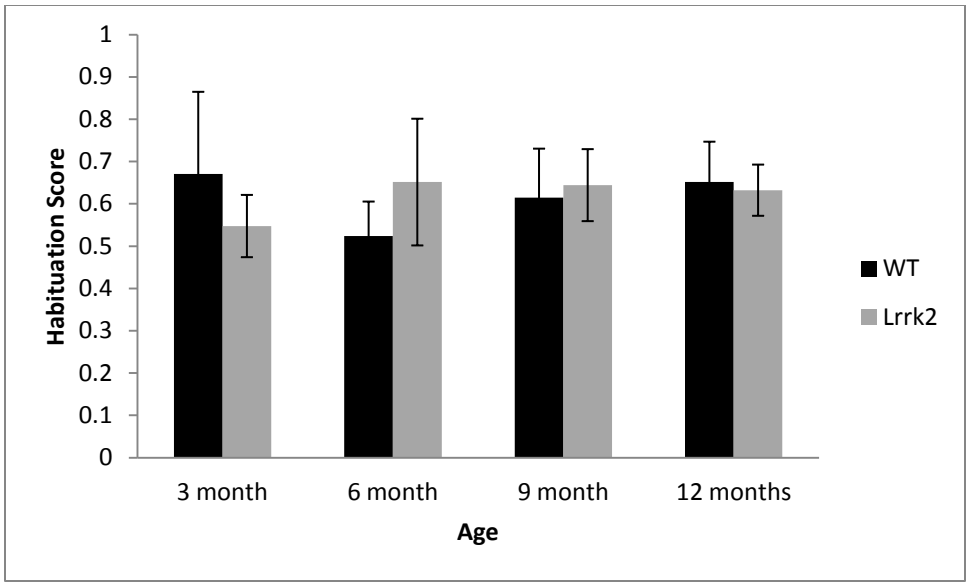

Figure 12: Habituation of the acoustic startle response.

Habituation scores were calculated for each rat by dividing the average of the last five startle responses by the maximum of the first three startle responses and then averaged across genotype. Habituation scores did not differ between transgenic *LRRK2*^{R1441G} rats and wildtype littermates at 3 (*LRRK2*^{R1441G}: M=0.55, SEM=0.07; WT: M=0.67, SEM=0.19), 6 (*LRRK2*^{R1441G}: M=0.65, SEM=0.15; WT: M=0.52, SEM=0.08), 9 (*LRRK2*^{R1441G}: M=0.64, SEM=0.09; WT:M=0.61, SEM=0.12), and 12 (*LRRK2*^{R1441G}: M=0.63, SEM=0.06; WT: M=0.65, SEM=0.10) months of age [ANOVA $F(3,102)=0.33$, $p=0.78$].

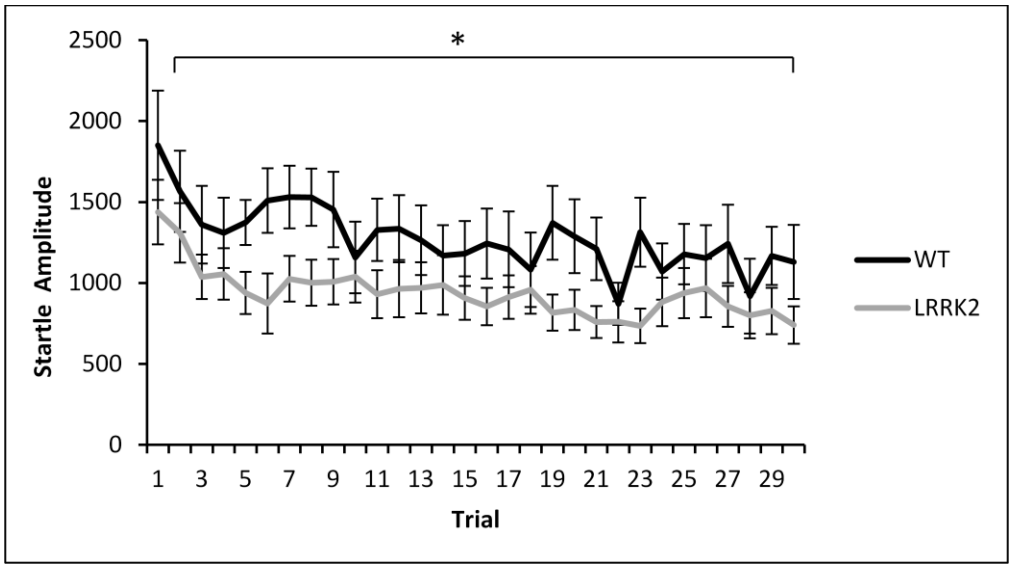

Figure 13: Habitation of the acoustic startle response at 3 months of age.

Startle amplitude was measured for each rat for 30 trials and then averaged by genotype. While the rats did show a decrease in responsiveness over time [ANOVA $F(16,643)=3.29$, $p<0.001$, Huynh-Feldt correction], there was no significant difference between transgenic *LRRK2*^{R1441G} rats and wildtype littermates [ANOVA $F(16, 643)=0.68$, $p=0.82$, Huynh-Feldt correction].

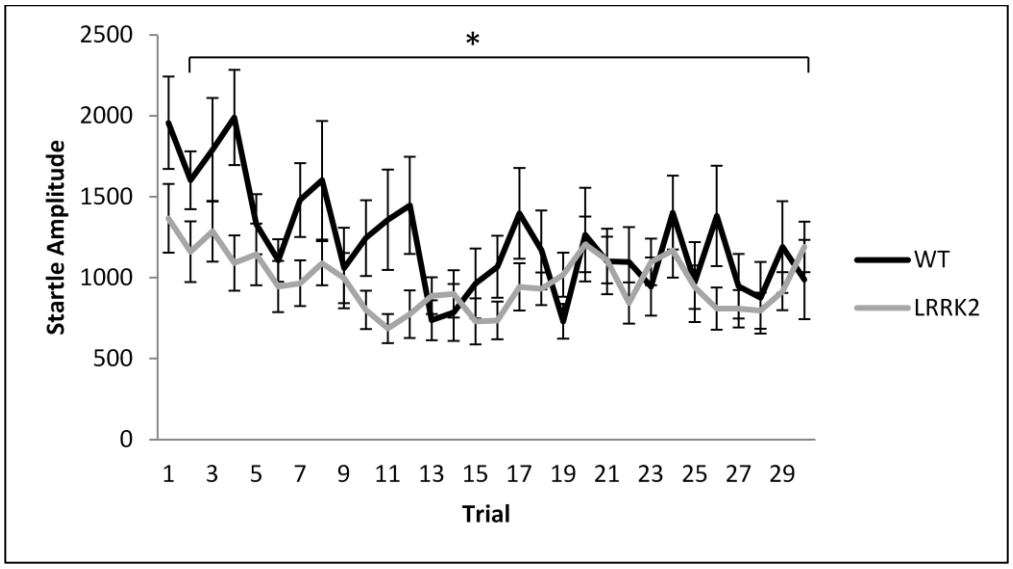

Figure 14: Habitation of the acoustic startle response at 6 months of age.

Startle amplitude was measured for each rat for 30 trials and then averaged by genotype. While the rats did show attenuation of the startle response [ANOVA $F(12,476)=2.85$, $p<0.001$, Huynh-Feldt correction], there was no significant difference between transgenic *LRRK2*^{R1441G} rats and wildtype littermates [ANOVA $F(12,476)=0.783$, $p=0.67$, Huynh-Feldt correction].

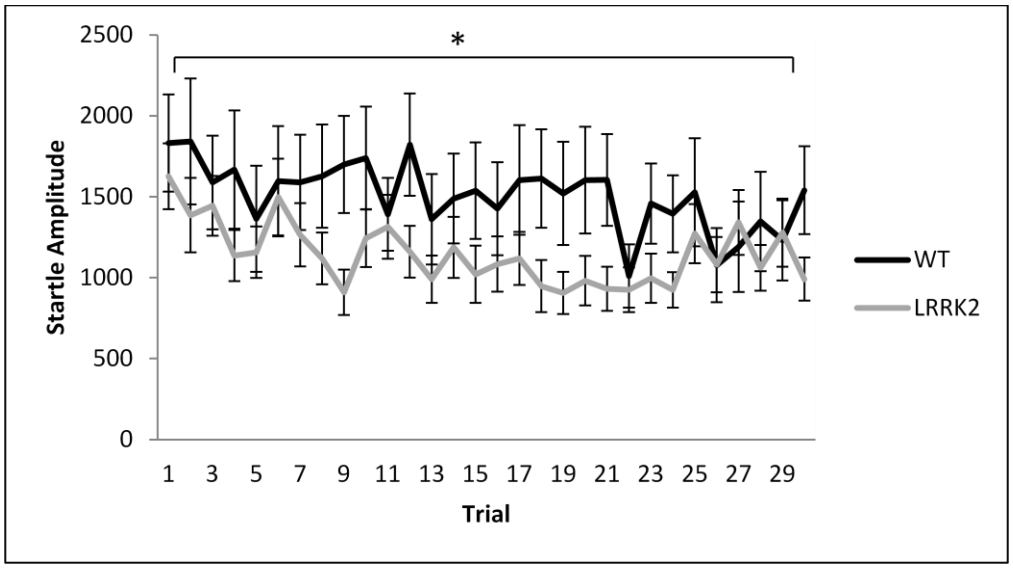

Figure 15: Habitation of the acoustic startle response at 9 months of age.

Startle amplitude was measured for each rat for 30 trials and then averaged by genotype. While the rats did show attenuation of the startle response [ANOVA $F(16,640)=1.91$, $p<0.05$, Huynh-Feldt correction], there was no significant difference between transgenic *LRRK2*^{R1441G} rats and wildtype littermates [ANOVA $F(16,640)=1.04$, $p=0.415$, Huynh-Feldt correction].

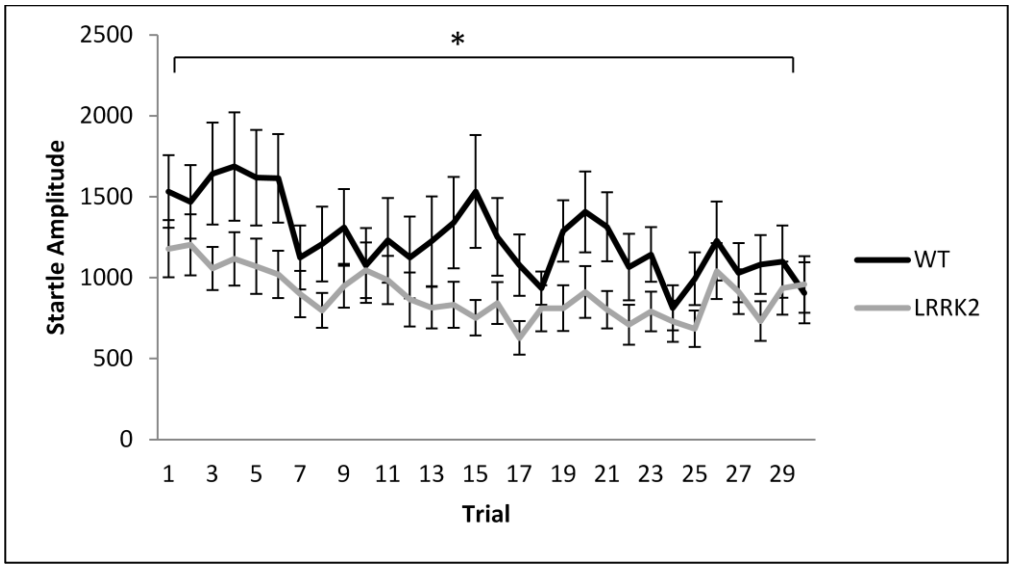

Figure 16: Habitation of the acoustic startle response at 12 months of age.

Startle amplitude was measured for each rat for 30 trials and then averaged by genotype. While the rats did show attenuation of the startle response [ANOVA $F(16,637)=2.97$, $p<0.001$, Huynh-Feldt correction], there was no significant difference between transgenic *LRRK2*^{R1441G} rats and wildtype littermates [ANOVA $F(16,637)=0.92$, $p=0.55$, Huynh-Feldt correction].

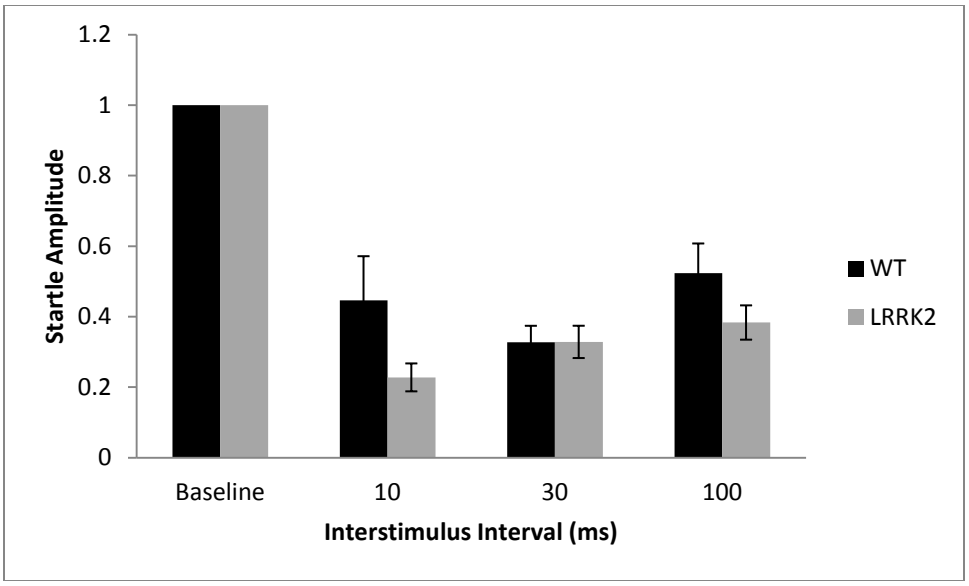

Figure 17: Prepulse inhibition of the acoustic startle response with 75 dB prepulse at 3 months of age.

Prepulse inhibition of the startle response was measured at three different interstimulus intervals: 10 ms, 30 ms, 100 ms. While all rats displayed prepulse inhibition of the startle response, there was no significant difference between transgenic *LRRK2*^{R1441G} rats and wildtype littermates at an ISI of 10 ms (*LRRK2*^{R1441G}: M=0.23, SEM=0.04; WT: M=0.45, SEM=0.13), 30 ms (*LRRK2*^{R1441G}: M=0.33, SEM=0.05; WT: M=0.33, SEM=0.05), and 100 ms [*LRRK2*^{R1441G}: M=0.38, SEM=0.05; WT:M=0.52, SEM=0.08; ANOVA $F(2,78)=0.64$, $p=0.53$].

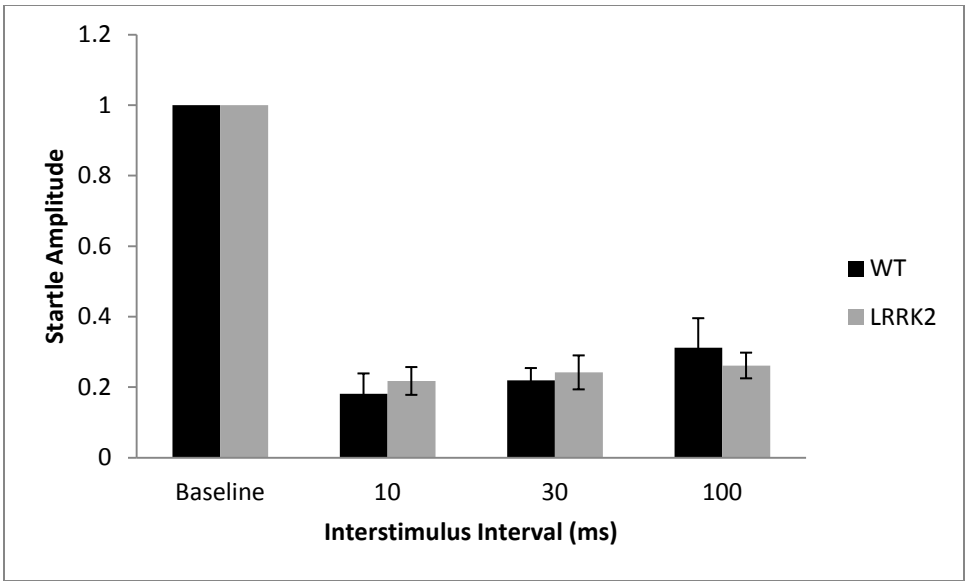

Figure 18: Prepulse inhibition of the acoustic startle response with 85 dB prepulse at 3 months of age.

Prepulse inhibition of the startle response was measured at three different interstimulus intervals: 10 ms, 30 ms, 100 ms. While all rats displayed prepulse inhibition of the startle response, there was no significant difference between transgenic *LRRK2*^{R1441G} rats and wildtype littermates at an ISI of 10 ms (*LRRK2*^{R1441G} M=0.22, SEM=0.04; WT: M=0.18, SEM=0.06), 30 ms (*LRRK2*^{R1441G} M=0.24, SEM=0.05; WT: M=0.22, SEM=0.04), and 100 ms [*LRRK2*^{R1441G} M=0.26, SEM=0.04; WT:M=0.31, SEM=0.08; $F(2,61)=0.228$, $p=0.74$; ANOVA $F(2,78)=0.64$, $p=0.53$].

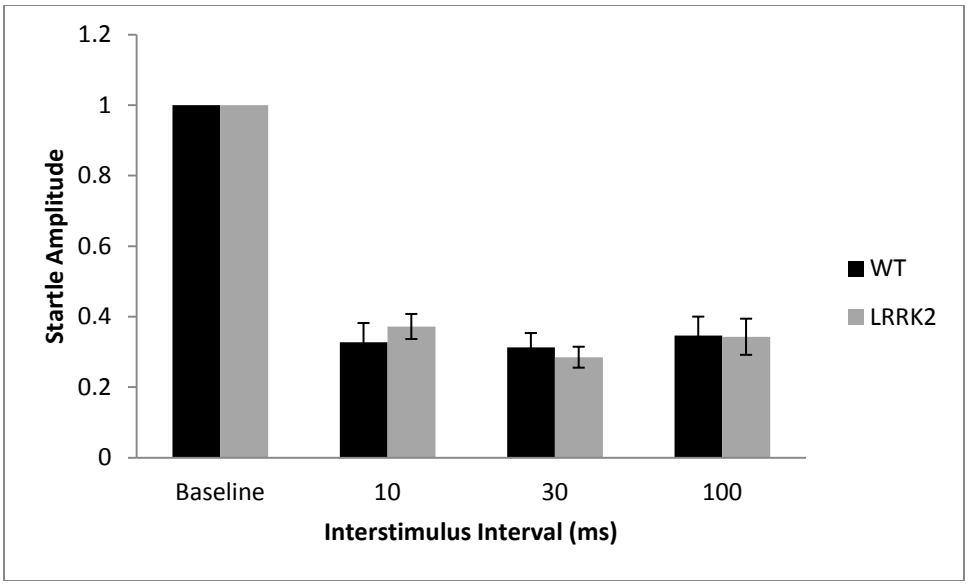

Figure 19: Prepulse inhibition of the acoustic startle response with 75 dB prepulse at 6 months of age.

Prepulse inhibition of the startle response was measured at three different interstimulus intervals: 10 ms, 30 ms, 100 ms. While all rats displayed prepulse inhibition of the startle response, there was no significant difference between transgenic *LRRK2*^{R1441G} rats and wildtype littermates at an ISI of 10 ms (*LRRK2*^{R1441G}: M=0.37, SEM=0.04; WT: M=0.33, SEM=0.05), 30 ms (*LRRK2*^{R1441G} M=0.28, SEM=0.03; WT: M=0.31, SEM=0.04), and 100 ms [*LRRK2*^{R1441G} M=0.34, SEM=0.05; WT:M=0.35, SEM=0.05; $F(2,61)=0.228$, $p=0.74$; ANOVA $F(2,61)=0.228$, $p=0.74$, Huynh-Feldt correction].

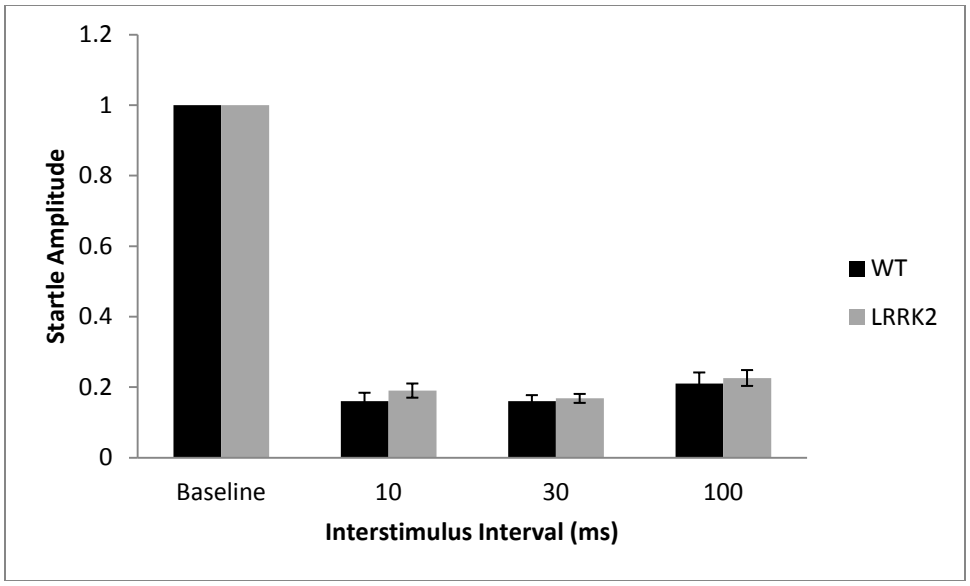

Figure 20: Prepulse inhibition of the acoustic startle response with 85 dB prepulse at 6 months of age.

Prepulse inhibition of the startle response was measured at three different interstimulus intervals: 10 ms, 30 ms, 100 ms. While all rats displayed prepulse inhibition of the startle response, there was no significant difference between transgenic *LRRK2*^{R1441G} rats and wildtype littermates at an ISI of 10 ms (*LRRK2*^{R1441G} M=0.19, SEM=0.02; WT: M=0.16, SEM=0.02), 30 ms (*LRRK2*^{R1441G} M=0.17, SEM=0.01; WT: M=0.16, SEM=0.01), and 100 ms [*LRRK2*^{R1441G} M=0.22, SEM=0.02; WT:M=0.21, SEM=0.03; $F(2,61)=0.228$, $p=0.74$;ANOVA $F(2,61)=0.228$, $p=0.74$, Huynh-Feldt correction].

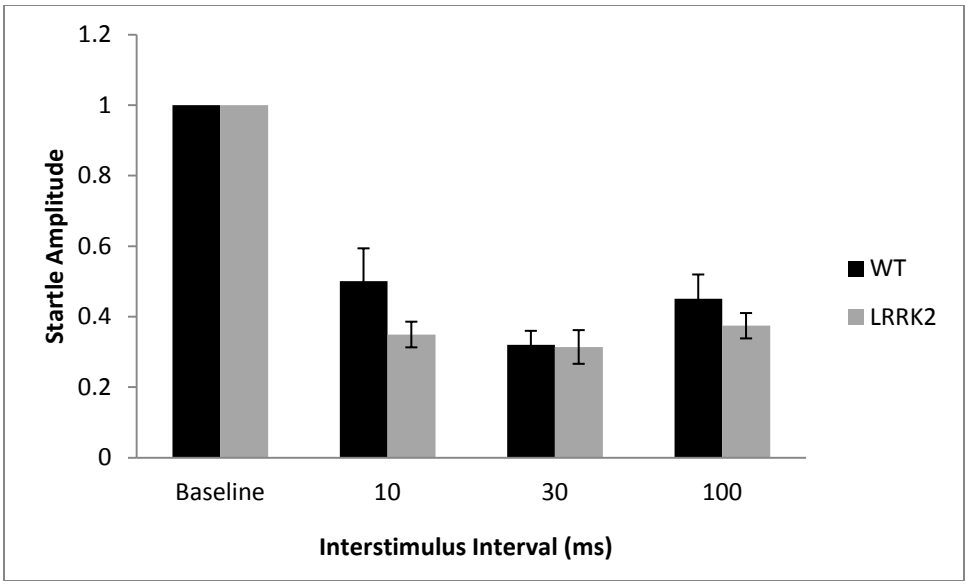

Figure 21: Prepulse inhibition of the acoustic startle response with 75 dB prepulse at 9 months of age.

Prepulse inhibition of the startle response was measured at three different interstimulus intervals: 10 ms, 30 ms, 100 ms. While all rats displayed prepulse inhibition of the startle response, there was no significant difference between transgenic *LRRK2*^{R1441G} rats and wildtype littermates at an ISI of 10 ms (*LRRK2*^{R1441G}: M=0.35, SEM=0.04; WT: M=0.50, SEM=0.09), 30 ms (*LRRK2*^{R1441G}: M=0.31, SEM=0.05; WT: M=0.32, SEM=0.04), and 100 ms [*LRRK2*^{R1441G}: M=0.37, SEM=0.04; WT:M=0.45, SEM=0.07; $F(2,61)=0.228$, $p=0.74$; ANOVA $F(2,78)=1.49$, $p=0.23$, Huynh-Feldt correction].

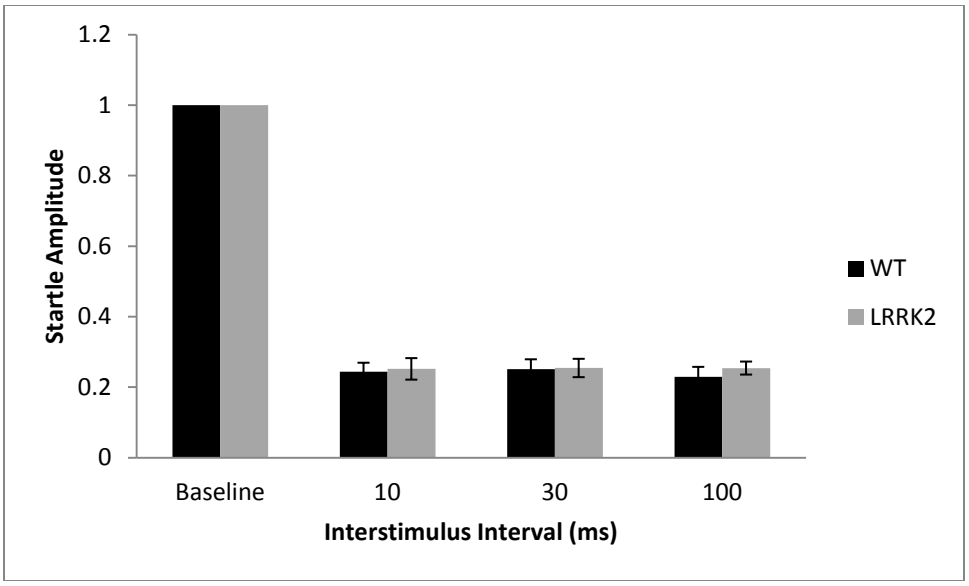

Figure 22: Prepulse inhibition of the acoustic startle response with 85 dB prepulse at 9 months of age.

Prepulse inhibition of the startle response was measured at three different interstimulus intervals: 10 ms, 30 ms, 100 ms. While all rats displayed prepulse inhibition of the startle response, there was no significant difference between transgenic *LRRK2*^{R1441G} rats and wildtype littermates at an ISI of 10 ms (*LRRK2*^{R1441G}: M=0.25, SEM=0.03; WT: M=0.24, SEM=0.03), 30 ms (*LRRK2*^{R1441G}: M=0.25, SEM=0.03; WT: M=0.25, SEM=0.03), and 100 ms [*LRRK2*^{R1441G}: M=0.25, SEM=0.02; WT:M=0.23, SEM=0.03; $F(2,61)=0.228$, $p=0.74$; ANOVA $F(2,78)=1.49$, $p=0.23$, Huynh-Feldt correction].

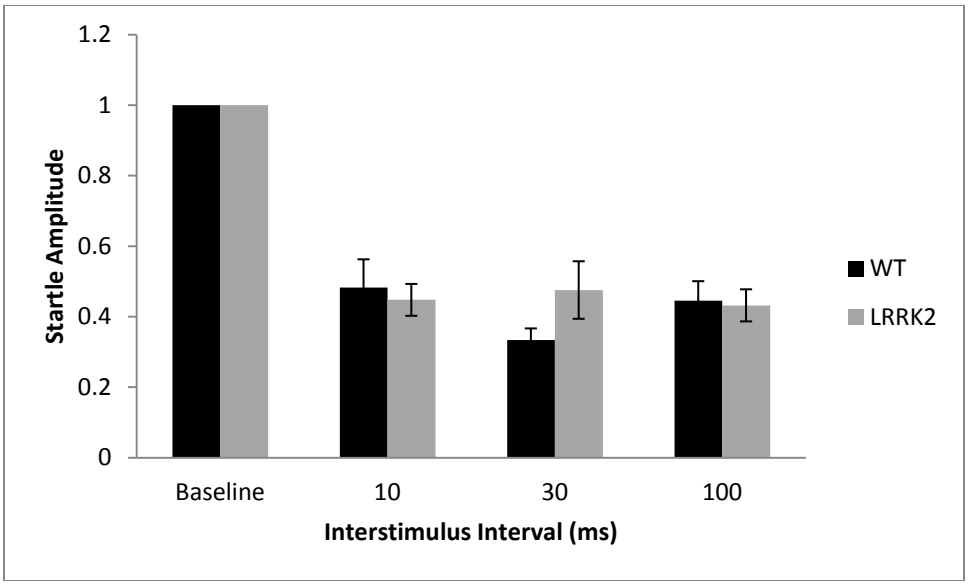

Figure 23: Prepulse inhibition of the acoustic startle response with 75 dB prepulse at 12 months of age.

Prepulse inhibition of the startle response was measured at three different interstimulus intervals: 10 ms, 30 ms, 100 ms. While all rats displayed prepulse inhibition of the startle response, there was no significant difference between transgenic *LRRK2*^{R1441G} rats and wildtype littermates at an ISI of 10 ms (*LRRK2*^{R1441G}: M=0.45, SEM=0.05; WT: M=0.48, SEM=0.08), 30 ms (*LRRK2*^{R1441G}: M=0.48, SEM=0.08; WT: M=0.33, SEM=0.03), and 100 ms [*LRRK2*^{R1441G}: M=0.43, SEM=0.05; WT:M=0.45, SEM=0.06; $F(2,61)=0.228$, $p=0.74$; ANOVA $F(2,78)=1.59$, $p=0.21$, Huynh-Feldt correction].

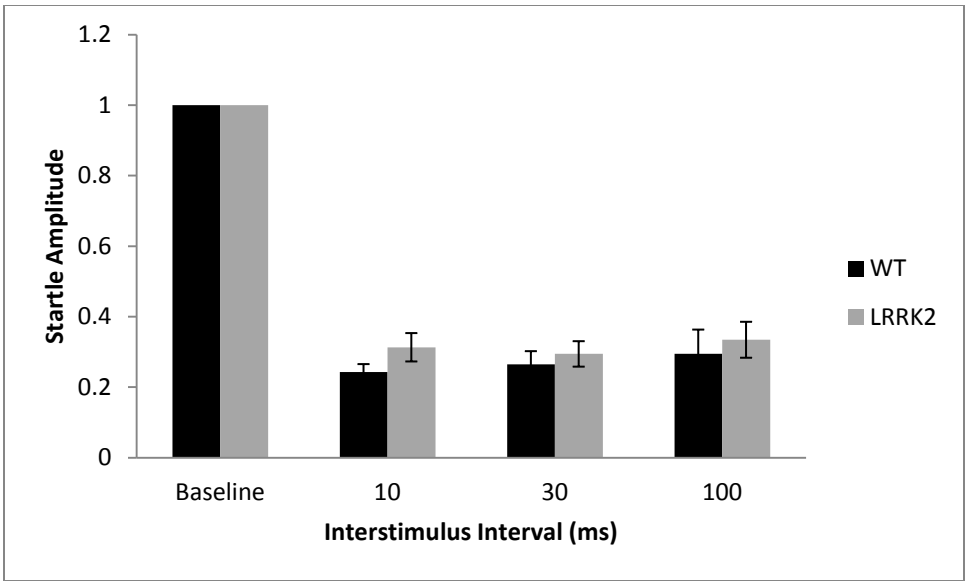

Figure 24: Prepulse inhibition of the acoustic startle response with 85 dB prepulse at 12 months of age.

Prepulse inhibition of the startle response was measured at three different interstimulus intervals: 10 ms, 30 ms, 100 ms. While all rats displayed prepulse inhibition of the startle response, there was no significant difference between transgenic *LRRK2*^{R1441G} rats and wildtype littermates at an ISI of 10 ms (*LRRK2*^{R1441G}: M=0.31, SEM=0.04; WT: M=0.24, SEM=0.02), 30 ms (*LRRK2*^{R1441G}: M=0.29, SEM=0.04; WT: M=0.26, SEM=0.04), and 100 ms [*LRRK2*^{R1441G}: M=0.33, SEM=0.05; WT:M=0.29, SEM=0.07; $F(2,61)=0.228$, $p=0.74$; ANOVA $F(2,78)=1.59$, $p=0.21$, Huynh-Feldt correction].

5.1.2.2 Morris Water Maze

All rats were tested on the Morris water maze in order to assess learning. In the cued version of the test, latency to find the escape platform improved over training days at 9 months [ANOVA $F(1,39)=31.73$, $p<0.001$, Huynh-Feldt correction; Figure 25] and 12 months of age [ANOVA $F(1,38)=7.11$, $p<0.05$, Huynh-Feldt correction; Figure 29]. However at both 9 months [ANOVA $F(1,39)=0.06$, $p=0.81$, Huynh-Feldt correction] and 12 months [ANOVA $F(1,38)=1.54$, $p=0.22$, Huynh-Feldt correction], there was no significant difference between transgenic *LRRK2*^{R1441G} rats and wildtype controls. In the spatial version of the test, training improved the mean latency to the platform in all rats at 9 [ANOVA $F(2,66)=13.6$, $p<0.001$, Huynh-Feldt correction; Figure 26] and 12 [ANOVA

F(3,102)=15.34, *p<0.001,* Huynh-Feldt correction; Figure 30] months of age, however no significant genotype difference was noted at either age point [9 months ANOVA *F*(2, 66)=0.93, *p=0.39,* Huynh-Feldt correction; 12 months ANOVA *F*(3,102)=1.09, *p=0.35,* Huynh-Feldt correction]. In the working memory version of the test, performance improved as a function of trials at 9 [ANOVA *F*(2,91)=9.7, *p<0.001,* Huynh-Feldt correction; Figure 27] months and 12 [ANOVA *F*(2,68)=3.72, *p<0.05,* Huynh-Feldt correction; Figure 31] months of age. However at 9 [ANOVA *F*(2, 91)=1.10, *p=0.34,* Huynh-Feldt correction] and 12 [ANOVA *F*(2, 68)=1.15, *p=0.32,* Huynh-Feldt correction] months of age, there was no significant difference between transgenic and wildtype animals. Finally, a probe trial was conducted at the end of testing to assess the amount of time spent in the target quadrant. At 9 months [t(39)=0.43, *p=0.67*; Figure 28] and 12 months [t(38)=0.30, *p=0.77*; Figure 32] months of age, there was no significant difference in time spent in target quadrant between transgenic *LRRK2*^{R1441G} rats and their wildtype littermates.

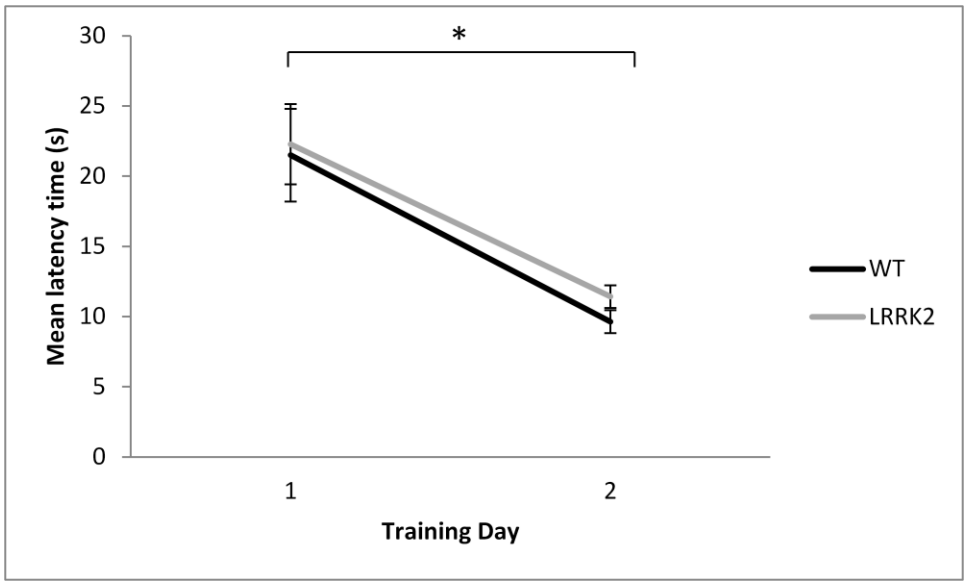

Figure 25: Cued Version of the Morris Water Maze task at 9 months of age.

Latency to find the target platform was measured across two training days in the cued version of the Morris water maze task. Performance on this task improved from training day 1 (*LRRK2*^{R1441G}: M=22.28, SEM=2.86; WT: M=21.49, SEM=3.30) to training day 2 (*LRRK2*^{R1441G}: M=11.42, SEM=0.80; WT: M=9.63, SEM=0.81) in all rats [ANOVA $F(1,39)=31.73$, $p<0.001$, Huynh-Feldt correction], however there was no significant difference between transgenic *LRRK2*^{R1441G} rats and wildtype controls [ANOVA $F(1,39)=0.06$, $p=0.81$, Huynh-Feldt correction].

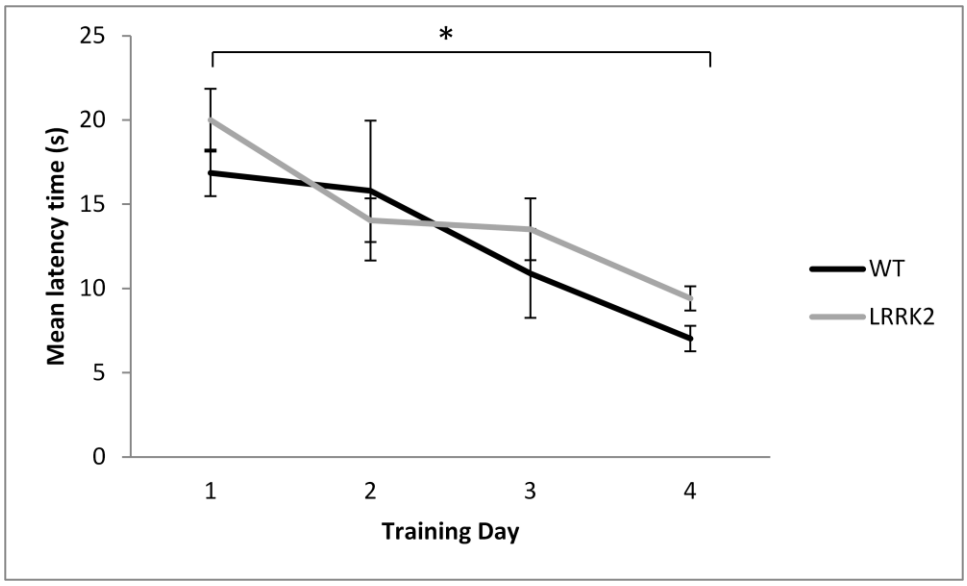

Figure 26: Spatial Reference Version of the Morris Water Maze task at 9 months of age.

Latency to find the target platform was measured across four training days in the cued version of the Morris water maze task. Performance on this task improved across training days (*LRRK2*^{R1441G}: M=9.40, SEM=0.71; WT: M=7.03, SEM=0.76) in all rats [ANOVA $F(2,66)=13.6$, $p<0.001$, Huynh-Feldt correction], however there was no significant difference between transgenic *LRRK2*^{R1441G} rats and wildtype controls [ANOVA $F(2, 66)=0.93$, $p=0.39$, Huynh-Feldt correction].

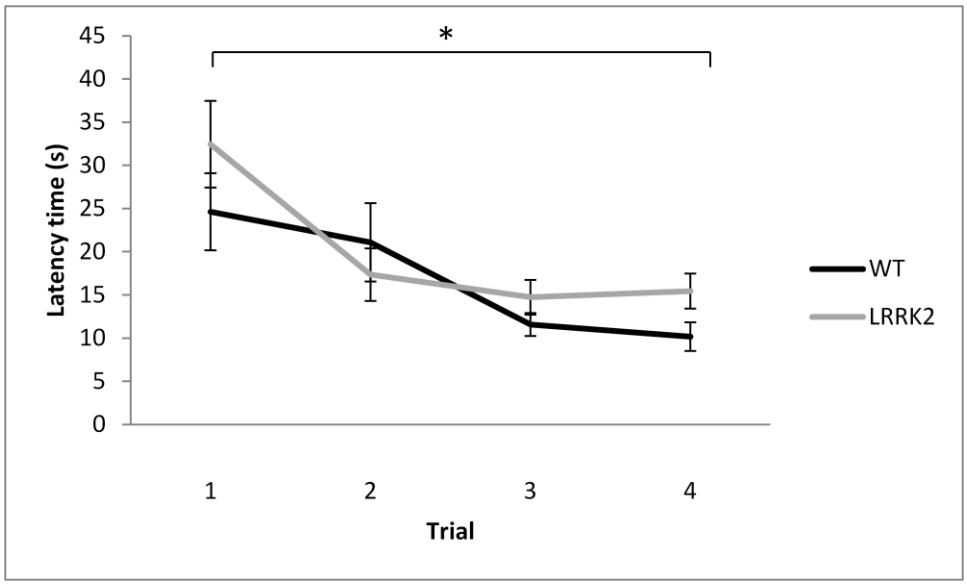

Figure 27: Working Memory Version of the Morris Water Maze task at 9 months of age.

Latency to find the target platform was measured across four consecutive trials on one day in the working memory version of the Morris water maze task. Performance on this task improved across trials (*LRRK2*^{R1441G}: M=15.45, SEM=2.04; WT: M=10.17, SEM=1.66) in all rats [ANOVA $F(2,91)=9.7$, $p<0.001$, Huynh-Feldt correction], however there was no significant difference between transgenic *LRRK2*^{R1441G} rats and wildtype controls [ANOVA $F(2, 91)=1.10$, $p=0.34$, Huynh-Feldt correction].

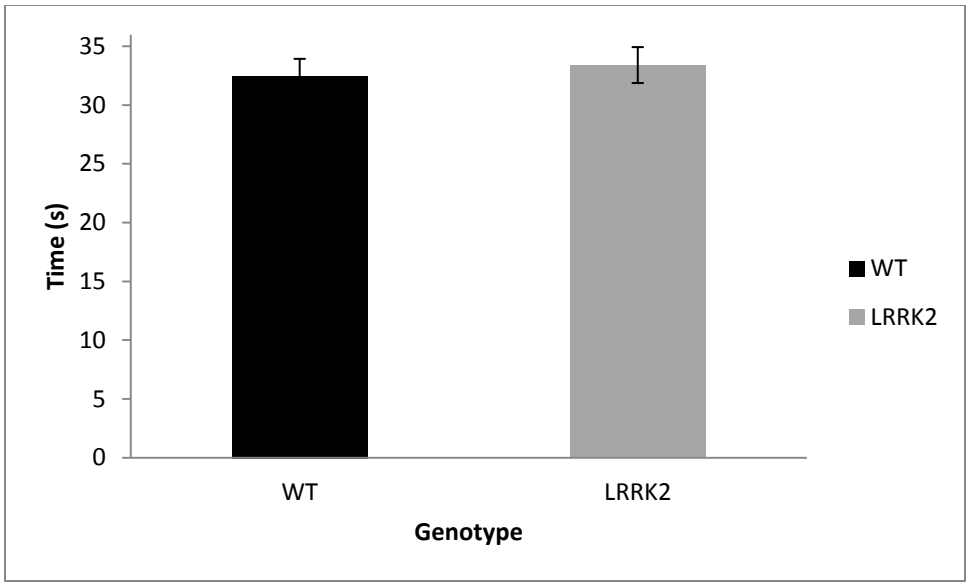

Figure 28: Probe Trial in the Morris Water Maze at 9 months of age.

Time spent in the target quadrant was measured in a probe trial in *LRRK2*^{R1441G} (M=33.41, SEM=1.53) and WT rats (M=32.46, SEM=1.47). There was no significant difference between the two genotypes [t(39)=0.43, *p=0.67*].

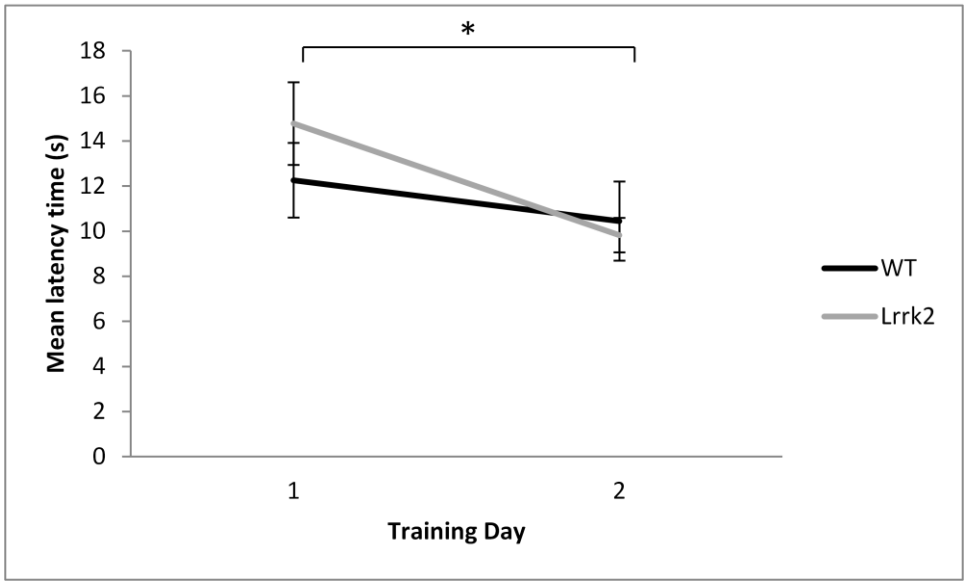

Figure 29: Cued Version of the Morris Water Maze task at 12 months of age.

Latency to find the target platform was measured across two training days in the cued version of the Morris water maze task. Performance on this task improved from training day 1 (*LRRK2*^{R1441G}: M=14.77, SEM=1.83; WT: M=12.26, SEM=1.65) to training day 2 (*LRRK2*^{R1441G}: M=9.83, SEM=0.77; WT: M=10.45, SEM=1.76) in all rats [ANOVA $F(1,38)=7.11$, $p<0.05$, Huynh-Feldt correction], however there was no significant difference between transgenic *LRRK2*^{R1441G} rats and wildtype controls [ANOVA $F(1,38)=1.54$, $p=0.22$, Huynh-Feldt correction].

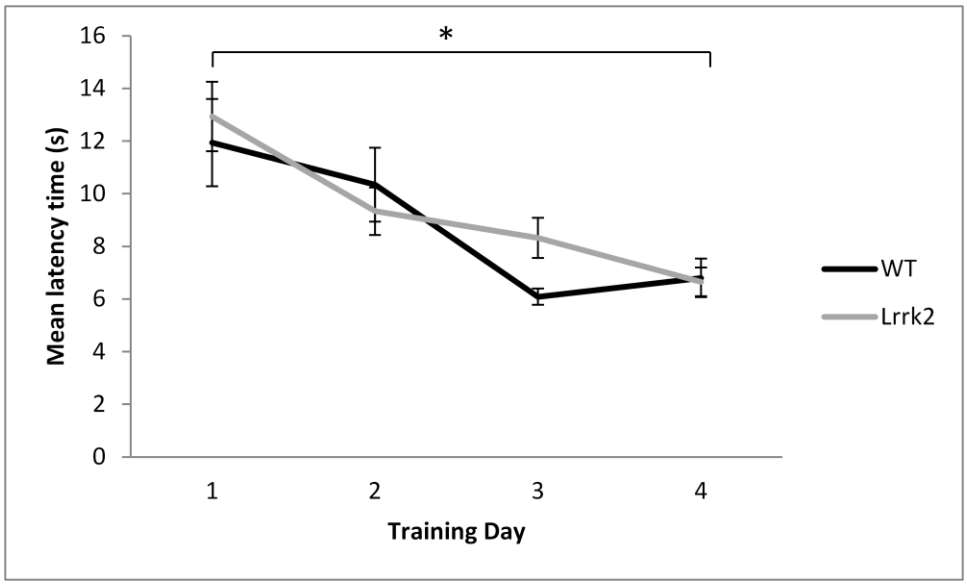

Figure 30: Spatial Reference Version of the Morris Water Maze task at 12 months of age.

Latency to find the target platform was measured across four training days in the cued version of the Morris water maze task. Performance on this task improved by training day 4 (*LRRK2*^{R1441G} M=6.65, SEM=0.55; WT: M=6.8, SEM=0.73) in all rats [ANOVA $F(3,102)=15.34$, $p<0.001$, Huynh-Feldt correction], however there was no significant difference between transgenic *LRRK2*^{R1441G} rats and wildtype controls [ANOVA $F(3,102)=1.09$, $p=0.35$, Huynh-Feldt correction].

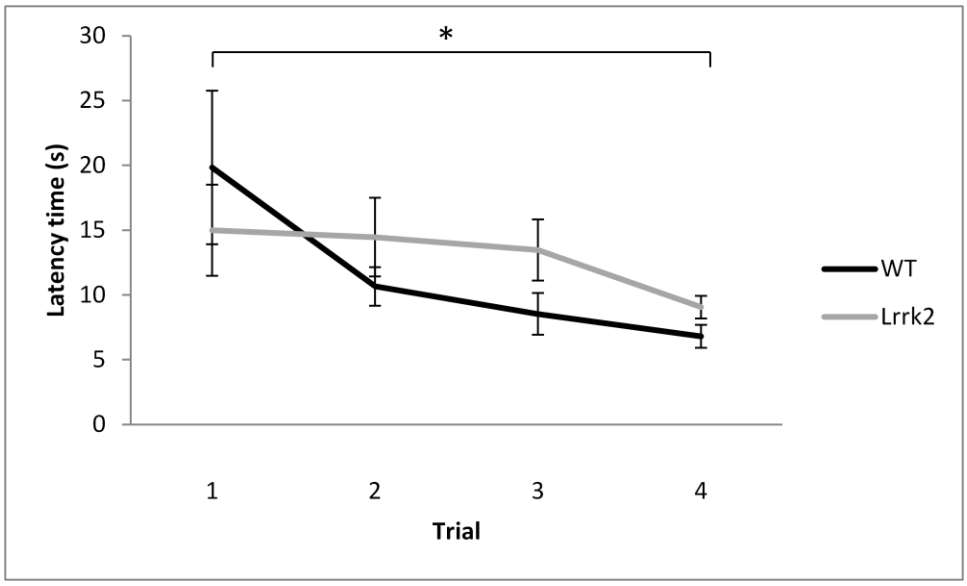

Figure 31: Working Memory Version of the Morris Water Maze task at 12 months of age.

Latency to find the target platform was measured across four consecutive trials on one day in the working memory version of the Morris water maze task. Performance on this task improved by the last trial (*LRRK2*^{R1441G} M=9.06, SEM=0.86; WT: M=6.8, SEM=0.88) in all rats [ANOVA $F(2,68)=3.72$, $p<0.05$, Huynh-Feldt correction], however there was no significant difference between transgenic *LRRK2*^{R1441G} rats and wildtype controls [ANOVA $F(2, 68)=1.15$, $p=0.32$, Huynh-Feldt correction].

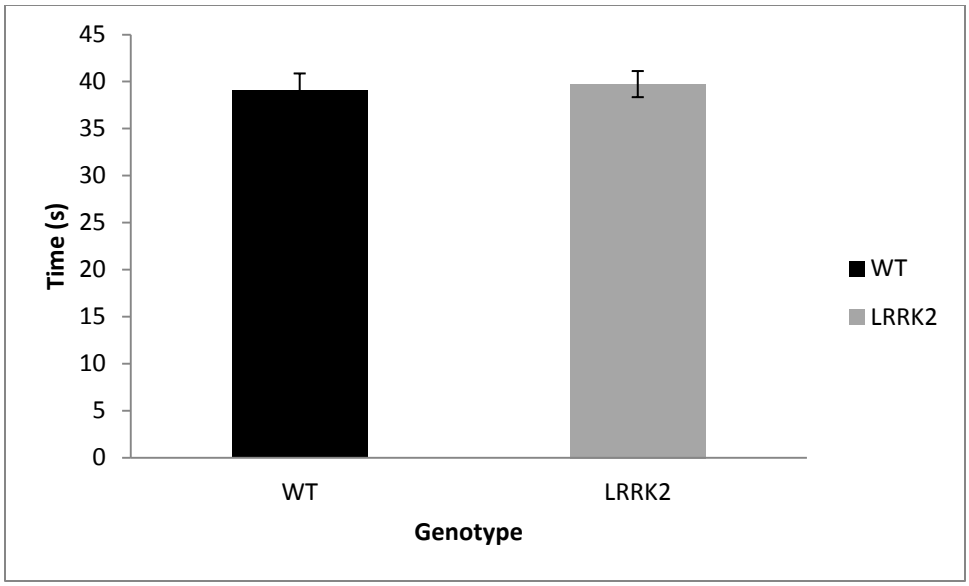

Figure 32: Probe Trial in the Morris Water Maze at 12 months of age.

Time spent in the target quadrant was measured in a probe trial in *LRRK2*^{R1441G} (M=39.73, SEM=1.39) and WT rats (M=39.06, SEM=1.80). There was no significant difference between the two genotypes [t(38)=0.30, *p=0.77*].

5.2 Study 2: Testing Paraquat Vulnerability in aged *LRRK2*^{R1441G} transgenic rats

In order to assess gene environment interactions in PD, vulnerability to Paraquat was measured in *LRRK2*^{R1441G} transgenic rats at approximately 14-16 months of age. Transgenic and wildtype rats were exposed to acute Paraquat poisoning and rearing behavior was recorded (Figure 33). Animals received two injections of Paraquat or saline and rearing behavior was measured immediately after each injection, 24 hours after each injection and ten days post injection. A significant reduction in rearing behavior over testing time points was noted in all animals [ANOVA $F(3, 83)=9.30$, $p<0.001$, Greenhouse-Geisser correction]. As expected, there was no overall main effect of drug, as a low dose of Paraquat was used in this experiment [ANOVA $F(3, 83)=2.50$, $p=0.83$, Greenhouse-Geisser correction]. There was no interaction between time, drug and genotype [ANOVA $F(3, 83)=0.30$, $p=0.83$, Greenhouse-Geisser correction]. Therefore, *LRRK2*^{R1441G} transgenic rats did not show vulnerability to Paraquat at the dose employed, as compared to wildtype controls. In addition, univariate ANOVA analysis was

conducted at each testing point. Immediately after injection 1, Paraquat exposed groups displayed significantly reduced rearing movements [ANOVA $F(1, 32)=5.51$, $p<0.05$], however the transgenic animals did not significantly differ from wildtype controls [ANOVA $F(1, 32)=0.033$, $p=0.857$]. This effect was lost 24 hours post injection 1, and no significant difference in rearing behavior was noted between groups exposed to Paraquat or saline [ANOVA $F(1, 28)=1.81$, $p=0.189$]. Immediately following injection 2, a significant main effect of drug was noted [ANOVA $F(1, 28)=8.45$, $p<0.05$], however again, there was no significant difference between transgenic and wildtype controls [ANOVA $F(1, 28)=0.23$, $p=0.64$]. 24 hours later, there was no difference between groups exposed to Paraquat or saline [ANOVA $F(1, 28)=2.73$, $p=0.06$]. Ten days post injection two, there was no significant main effect of drug [ANOVA $F(1, 28)=1.10$, $p=0.30$] or a genotype and drug interaction [ANOVA $F(1, 28)=0.37$, $p=0.55$]. Overall, although Paraquat had a short term effect on rearing behavior immediately following injections, this effect was not selective for *LRRK2*^{R1441G} rats, and was negated by ten days post injection. Kaplan-Meier curves and a log rank (Mantel-Cox) test were conducted to investigate survival estimates in transgenic *LRRK2*^{R1441G} and wildtype rats (Figure 34). There was no significant difference in survival time between transgenic and wildtype animals [$X^2(1)=2.65$, p=0.10]. Quantitative RT-PCR was conducted on surviving transgenic animals at 18 months of age. Initial genotyping had revealed a genomic presence of human *LRRK2* (Figure 35), however RT-PCR results performed in surviving transgenic rats at the end of the study revealed no detectable expression of human *LRRK2* in the substantia nigra, cortex, hippocampus, liver or kidney (Table 1).

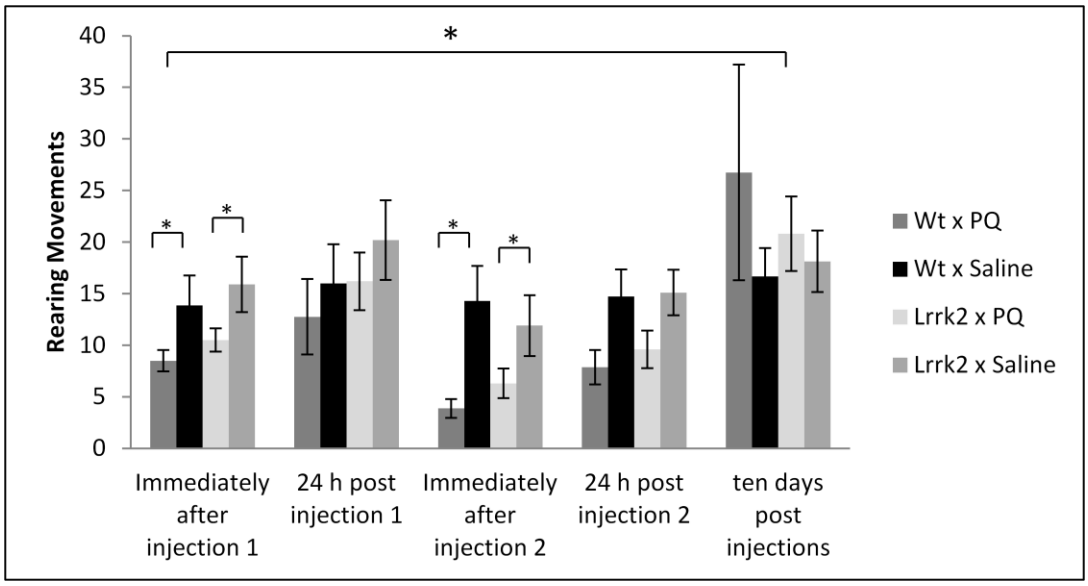

Figure 33: Vulnerability to acute Paraquat poisoning.

Rearing behavior following acute Paraquat poisoning or exposure to saline was measured in *LRRK2*^{R1441G} and wildtype rats. All animals were tested immediately after injection 1, 24 hours after injection 1, immediately after injection 2, 24 hours after injection 2 and ten days after the last injection. Overall, there was no significant interaction between drug and genotype [ANOVA $F(3, 83)=0.30$, $p=0.83$, Greenhouse-Geisser correction]. Univariate ANOVA was conducted to investigate time point specific trends. Immediately following injection 1 [ANOVA $F(1, 32)=5.51$, $p<0.05$] and injection 2 [ANOVA $F(1, 28)=8.45$, $p<0.05$], there was a reduction in rearing movements in Paraquat-exposed groups. However, this trend was not specific to *LRRK2*^{R1441G} transgenic rats [injection 1 ANOVA $F(1, 32)=0.033$, $p=0.857$;injection 2 ANOVA $F(1, 28)=0.23$, $p=0.64$] and was negated 24 hours post injection [injection 1 ANOVA $F(1, 28)=1.81$, $p=0.189$; injection 2 ANOVA $F(1, 28)=2.73$, $p=0.06$]. Ten days following injections, no main effect of drug [ANOVA $F(1, 28)=1.10$, $p=0.30$] or genotype drug interaction [ANOVA $F(1, 28)=0.37$, $p=0.55$] in rearing behavior was noted.

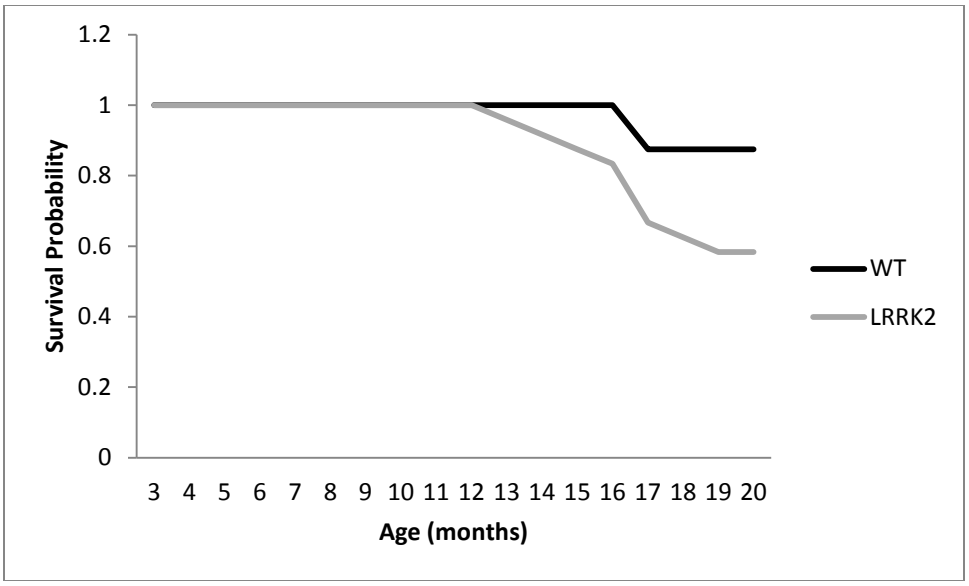

Figure 34: Survival curve for transgenic and wildtype rats.

Survival estimates were generated for *LRRK2*^{R1441G} (M=17.91, SEM=0.38) and WT rats (M=18.75, SEM=0.17). A log rank (Mantel-Cox) test revealed no significant differences in survival between transgenic and wildtype animals [$X^2(1)=2.65$, $p=0.10$].

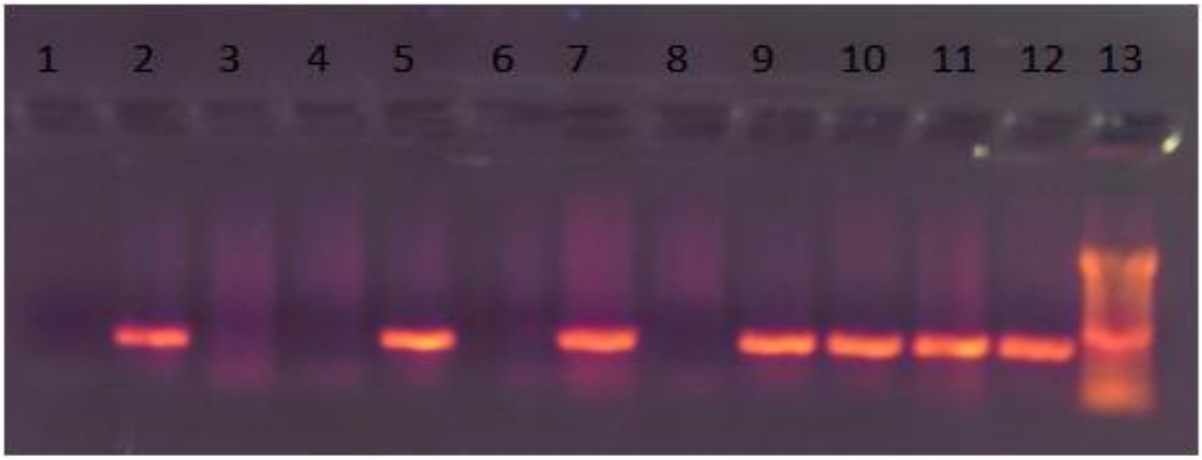

Lane	Sample
1	Negative Control
2	Positive Control
3	WT rat
4	WT rat
5	Tg *LRRK2*^{R1441G} rat
6	WT rat
7	Tg *LRRK2*^{R1441G} rat
8	WT rat
9	Tg *LRRK2*^{R1441G} rat
10	Tg *LRRK2*^{R1441G} rat
11	Tg *LRRK2*^{R1441G} rat
12	Tg *LRRK2*^{R1441G} rat
13	Ladder

Figure 35: **Genotype results for wildtype and transgenic animals.**

Genotype results show positive bands, indicating presence of human *LRRK2*, as compared to wildtype rats which do not express human *LRRK2*.

Animal ID	Genotype	DOB	Tissue	LRRK2 expression		GAPDH expression	
				Mean	SD	Mean	SD
101		7/26/2012	Hippocampus	-	-	17.808	0.203
			Substantia Nigra	-	-	18.217	0.287
			Cortex	-	-	21.133	0.212
			Kidney	-	-	19.127	0.142
			Liver	-	-	18.912	0.096
102		7/26/2012	Hippocampus	-	-	18.730	0.169
			Substantia Nigra	-	-	19.639	0.025
			Cortex	-	-	17.477	0.581
			Kidney	-	-	18.105	0.372
			Liver	-	-	18.790	0.161
104		7/26/2012	Hippocampus	-	-	18.897	0.928
			Substantia Nigra	-	-	21.802	4.886
			Cortex	-	-	19.578	0.121
			Kidney	-	-	19.308	0.360
			Liver	-	-	22.004	0.194
102		7/26/2012	Hippocampus	-	-	18.730	0.169
			Substantia Nigra	-	-	19.639	0.025
			Cortex	-	-	17.477	0.581
			Kidney	-	-	18.105	0.372
			Liver	-	-	18.790	0.161
104		7/26/2012	Hippocampus	-	-	18.897	0.928
			Substantia Nigra	-	-	21.802	4.886

		Cortex	-	-	19.578	0.121
		Kidney	-	-	19.308	0.360
		Liver	-	-	22.004	0.194
303	8/5/2012	Hippocampus	-	-	20.458	0.347
		Substantia Nigra	-	-	20.347	0.961
		Cortex	-	-	19.271	0.261
		Kidney	-	-	18.998	1.423
		Liver	-	-	21.391	0.311
305	8/5/2012	Hippocampus	-	-	19.391	0.287
		Substantia Nigra	-	-	20.340	1.455
		Cortex	-	-	19.271	0.261
		Kidney	-	-	18.901	0.102
		Liver	-	-	21.164	0.351
404	9/16/2012	Hippocampus	-	-	19.710	0.153
		Substantia Nigra	-	-	20.246	0.051
		Cortex	-	-	19.144	0.567
		Kidney	-	-	20.316	0.669
		Liver	-	-	23.021	3.470
406	9/16/2012	Hippocampus	-	-	21.827	5.225
		Substantia Nigra	-	-	20.121	0.083
		Cortex	-	-	18.711	0.251
		Kidney	-	-	19.768	0.282
		Liver	-	-	22.133	0.081
502	9/25/2012	Hippocampus	-	-	18.933	0.103

		Substantia Nigra	-	-	20.223	0.550
		Cortex	-	-	20.541	0.069
		Kidney	-	-	19.134	0.029
		Liver	-	-	21.181	0.335
503	9/25/2012	Hippocampus	-	-	23.215	0.079
		Substantia Nigra	-	-	24.910	0.151
		Cortex	-	-	23.557	0.258
		Kidney	-	-	25.013	3.874
		Liver	-	-	20.843	0.110
506	9/25/2012	Hippocampus	-	-	18.746	0.283
		Substantia Nigra	-	-	18.474	0.085
		Cortex	-	-	21.564	0.106
		Kidney	-	-	28.604	0.233
		Liver	-	-	21.927	0.899
703	9/29/2012	Hippocampus	-	-	21.522	0.130
		Substantia Nigra	-	-	34.326	0.436
		Cortex	-	-	21.379	0.127
		Kidney	-	-	26.567	0.194
		Liver	-	-	23.392	0.092

Table 1: qRT-PCR expression of wildtype and transgenic animals.

No detectable expression of human *LRRK2* in surviving transgenic *LRRK2*^{R1441G} rats in the hippocampus, substantia nigra, cortex, kidney or liver was noted.

Chapter 6

6 Discussion

6.1 Introduction

Animal models are critical tools for not only understanding LRRK2 pathobiology but also PD aetiology and pathogenesis. In particular, models which carry PD related mutations on the human *LRRK2* gene can provide insight into LRRK2 function and the mechanisms by which it mediates PD related dysfunction. Recently, bacterial artificial chromosome (BAC) *LRRK2* transgenic rodent models have been generated which allow us to investigate the link between genetic mutations and development of PD. Here we have characterized transgenic *LRRK2*^{R1441G} BAC rats. These rats do not display PD related motor or cognitive deficits by 12 months of age, and do not show increased vulnerability to Paraquat poisoning as compared to age-matched wildtype controls.

6.2 Evidence from other transgenic models of LRRK2 mediated PD

Although to our knowledge no previous studies have examined PD phenotypes in *LRRK2*^{R1441G} transgenic BAC rats, our results are supported by recent studies in which transgenic *LRRK2* BAC mice fail to consistently reproduce cardinal features of PD. Although Li et al. (2009) originally reported age-dependent, L-DOPA responsive, progressive motor dysfunction in *LRRK2*^{R1441G} BAC mice by 10 months of age, subsequent studies in transgenic mice have been unable to reproduce these results. Bichler et al. (2013) did not observe gross motor dysfunction in transgenic *LRRK2*^{R1441G} BAC mice by 10 months of age, although modest motor deficits were observed in advanced age (21 months of age). These mice also did not display cognitive symptoms of PD, including depression and anxiety-like behaviour and impaired learning and memory (Bichler et al., 2013). However, gastrointestinal dysfunction, a common early non-motor symptom of PD was noted in these mice by 6 months of age (Bichler et al., 2013). Dranka et al. (2013) did not report gross motor abnormalities in *LRRK2*^{R1441G} BAC mice, although by 16 months of age, these mice did display deficits in motor coordination, an early symptom of PD. Similarly, other classic transgenic *LRRK2* mouse models have

failed to show PD specific gross motor deficits (Li et al., 2010; Melrose et al., 2010; Ramonet et al., 2011). The mild impairment of motor function seen in transgenic mice models is further supported by the fact that these lines lack degeneration of nigrostriatal dopaminergic neurons, although impaired dopaminergic neurotransmission was observed (Li et al., 2009; Tong et al., 2009; Melrose et al., 2010; Dranka et al., 2013). Taken together, these results suggest that transgenic *LRRK2* rodents at best model early phenotypes of Parkinson disease and do not recapitulate late stage PD phenotypes, including the motor and cognitive deficits tested here.

6.3 Limitations of the Model

Parkinson disease is characterized by slow and progressive degeneration of the substantia nigra and disruption of basal ganglia circuitry with advancing age. While neurotoxin models which display disease outcomes have had great success in rats, the relatively short life span of rats as compared to humans may make them imperfect models for studying genetic forms of PD. A healthy laboratory rat can survive for approximately 3 years while LRRK2 mediated PD is not apparent in humans until after 65 years of age. Indeed, despite the discovery of many genetic mutations, the greatest known risk factor for PD continues to be advanced age. The rats used in this study were 12 months of age, which is considered ‘advanced’ age for rats (Quinn, 2005) but may not have been sufficient to reproduce PD related phenotypes. Some researchers have argued that high levels of transgene expression can induce neurological phenotypes within the life span of a rat. Ramonet et al. (2011) tested four different transgenic mouse lines, expressing either the G2019S mutation or the R1441C mutation and observed neuronal loss in advanced age in only one line, in which transgene expression was more than 300% greater than the level of endogenous LRRK2. However, in this case non-physiological levels of transgene expression are used which while producing PD phenotypes may limit our ability to translate animal research to human disease.

In addition, it is possible that because the transgene was constitutively expressed in these rats, they were able to develop compensatory mechanisms which counteracted the toxic effects of mutated LRRK2. Zhou et al (2011) found no behavioural phenotypes in rats that constitutively expressed mutated LRRK2 however they did observe abnormal motor

activity in rats with conditional adult onset expression of mutated LRRK2. Their results suggest that rats are able to accommodate LRRK2's toxic effects when it is constitutively expressed. With this in mind, it is possible that future genetic models of PD should consider the viral mediated gene transfer approach instead of the BAC approach. With the viral mediated gene transfer approach, the mutated *LRRK2* gene can be delivered to rodents through a viral vector in adulthood, thus bypassing the development of compensatory effects. This approach also allows researchers to target specific neuronal populations, such as susbtantia nigra dopaminergic neurons, to better model the degeneration seen in PD. Another advantage of the viral mediated gene transfer approach is that it allows researchers to correlate transgene dosage (by modulating copy number of transgene) with phenotype severity. Studies using this approach have already had success in recapitulating cardinal features of PD. Lee et al (2010) created a mouse model of PD expressing human G2019S LRRK2 using herpes simplex virus (HSV), which displayed 50% degeneration of nigral dopaminergic neurons. In addition a rat model generated by Dusonchet et al (2011) expressing human G2019S LRRK2 showed a 20% reduction in dopaminergic neurons. Viral models may allow us to recapitulate neurodegeneration observed in PD patients, which has thus far been difficult to show in transgenic BAC models.

6.4 Multiple Hit Hypothesis of PD

This study also explored the 'multiple hit' hypothesis of PD by investigating the vulnerability of *LRRK2*^{R1441G} transgenic rats to Paraquat poisoning. We exposed both transgenic and wildtype rats to a low, acute dose of Paraquat exposure, in order to examine synergistic effects of genetic mutations and environmental toxins on PD development. As expected, the low dose of Paraquat used in this study did not have lasting effects on rearing behaviour. Unexpectedly, transgenic rats did not differ from wildtype controls in rearing behaviour following acute Paraquat exposure, suggesting a lack of gene environment interaction between *LRRK2* and Paraquat. Therefore, these results did not provide support for the 'multiple hit' hypothesis. Nevertheless, a dose-reponse study with higher doses would be necessary before this hypothesis can be discounted. Our results are inconsistent with previous studies which show an interaction

between PD-related mutations in the SNCA gene and environmental exposure in mediating PD risk (Peng et al., 2010; Desplats et al., 2012; Nuber et al., 2014). Currently, few studies have investigated gene environment interactions using PD related mutations in the *LRRK2* gene. However, one group did note altered transcriptional regulation of neurogenesis related genes upon exposure to Paraquat in *LRRK2*^{G2019S} mice (Desplats et al., 2012). In addition, Ray et al (2014) found enhanced neurodegeneration when C. elegans DA neurons expressing human α-syn or LRRK2 (G2019S) were exposed to a bacterial metabolite. Alternatively, an epidemiological study by Chung et al. (2013) did not find an interaction between environmental exposure and *LRRK2* genes. Our results in the context of previous literature suggest that further investigation is necessary in order to confirm the interaction between PD-related *LRRK2* mutations and environmental exposure. One explanation is that previous animal studies have largely looked at neuropathology and have not examined motor dysfunction. As previously mentioned, significant neurodegeneration is necessary before the onset of motor symptoms. It is possible that our rats simply did not develop motor symptoms at the time of testing and that continued exposure to Paraquat would have induced a motor phenotype in *LRRK2*^{R1441G} rats. The Paraquat paradigm used in this experiment was modeled after an earlier study investigating the interaction between traumatic brain injury and exposure to Paraquat (Hutson et al., 2011). This study reported a robust interaction between traumatic brain injury and Paraquat exposure on rearing behaviour in rats. However, it is possible that because our LRRK2 mutation did not cause neurodegeneration to the extent described in the TBI rats (Hutson et al., 2011), a more lethal dose of Paraquat was required to induce PD related motor phenotypes.

6.5 Methodological Considerations

An important methodological limitation of this study is that there were no detectable levels of transgene expression in surviving *LRRK2*^{R1441G} transgenic rats. While transgenic rats did display genomic *LRRK2* in initial genotyping PCR results, this gene seemed to be not transcribed to a detectable level as displayed by quantitative RT-PCR results. One limitation of the transgenic approach is that due to random integration of the transgene, positional effects can occur. Position effects refer to the phenomenon whereby transgene

expression is influenced by the integration site. BAC constructs are large genomic inserts and due to their size (~200 kb) allow the inclusion of endogenous regulatory elements, which should greatly reduce the probability of position effects. However the lack of transgene expression noted in this model suggests that transgene insertion, even with the BAC approach, was not stable. Position effects can include lack of transgene expression and extinction of transgene expression in successive generations. As the rats tested in this study were bred from an original pair obtained from Taconic, it is possible that transgene expression diminished due to successive breeding. Another consideration is that only rats which survived until the end of the study were tested for transgene expression. Indeed the animals most likely to show levels of transgene expression were those who did not survive after the administration of Paraquat as it is possible that insertion of the *LRRK2* gene impacted viability. Interestingly, post-mortem analysis conducted on *LRRK2* rats which did not survive until the end of the study indicates morphology consistent with hemopoietic tumors. A recent study by Ruiz-Martinez et al (2014) reported a higher prevalence of hematological cancers in patients carried the R1441G mutation.

6.6 Summary of findings

In this study, we characterized transgenic BAC rats carrying the R1441G mutation on the human *LRRK2* gene. Rats underwent motor and cognitive tests in order to assess the variety of behavioural phenotypes observed in Parkinson disease. Transgenic $LRRK2^{R1441G}$ rats did not display any motor or cognitive deficits reminiscent of Parkinson disease by 12 months of age. These results are consistent with studies performed on transgenic mice which also fail to reproduce gross motor abnormalities (Li et al., 2010; Melrose et al., 2010; Ramonet et al., 2011; Bichler et al., 2013; Dranka et al., 2013). Together these results suggest that the genetic mutation itself is insufficient to reproduce PD phenotypes in these rats. Also, transgenic $LRRK2^{R1441G}$ rats were tested for vulnerability to Paraquat poisoning, in order to assess the hypothesis that exposure to environmental toxins works synergistically with a genetic predisposition to PD to produce disease phenotypes. Our results show that $LRRK2^{R1441G}$ rats did not display increased vulnerability to the neurotoxin Paraquat, as compared to wildtype controls. This may be due to the low dose of Paraquat used in this study and the lack of transgene

expression. Overall, our results indicate that these transgenic BAC *LRRK2*^{R1441G} rats are not a viable model of Parkinson disease.

References

1. Alcalay RN, Caccappolo E, Mejia-Santana H, Tang MX, Rosado L, Ross BM, et al. Frequency of known mutations in early-onset parkinson disease. implication for genetic counseling: The consortium on risk for early onset parkinson disease study. Arch Neurol. 2010;67(9):1116-22.
2. Alegre-Abarrategui J, Christian H, Lufino MM, Mutihac R, Venda LL, Ansorge O, et al. LRRK2 regulates autophagic activity and localizes to specific membrane microdomains in a novel human genomic reporter cellular model. Hum Mol Genet. 2009 Nov 1;18(21):4022-34.
3. Allen MT, Levy LS. Parkinson's disease and pesticide exposure--a new assessment. Crit Rev Toxicol. 2013 Jul;43(6):515-34.
4. Anand VS, Braithwaite SP. LRRK2 in parkinson's disease: Biochemical functions. FEBS J. 2009 Nov;276(22):6428-35.
5. Andres-Mateos E, Mejias R, Sasaki M, Li X, Lin BM, Biskup S, et al. Unexpected lack of hypersensitivity in LRRK2 knock-out mice to MPTP (1-methyl-4-phenyl-1,2,3,6-tetrahydropyridine). J Neurosci. 2009 Dec 16;29(50):15846-50.
6. Anfossi M, Colao R, Gallo M, Bernardi L, Conidi ME, Frangipane F, et al. Identification of three novel LRRK2 mutations associated with parkinson's disease in a calabrian population. J Alzheimers Dis. 2014;38(2):351-7.
7. Baldereschi M, Di Carlo A, Vanni P, Ghetti A, Carbonin P, Amaducci L, et al. Lifestyle-related risk factors for parkinson's disease: A population-based study. Acta Neurol Scand. 2003;108(4):239-44.
8. Berg D, Schweitzer KJ, Leitner P, Zimprich A, Lichtner P, Belcredi P, et al. Type and frequency of mutations in the LRRK2 gene in familial and sporadic parkinson's disease*. Brain. 2005 Dec;128(Pt 12):3000-11.
9. Bernheimer H, Birkmayer W, Hornykiewicz O, Jellinger K, Seitelberger F. Brain dopamine and the syndromes of parkinson and huntington. clinical, morphological and neurochemical correlations. J Neurol Sci. 1973 Dec;20(4):415-55.
10. Berwick DC, Harvey K. LRRK2 signaling pathways: The key to unlocking neurodegeneration? Trends Cell Biol. 2011 May;21(5):257-65.

11. Bichler Z, Lim HC, Zeng L, Tan EK. Non-motor and motor features in LRRK2 transgenic mice. PLoS One. 2013 Jul 30;8(7):e70249.
12. Biosa A, Trancikova A, Civiero L, Glauser L, Bubacco L, Greggio E, et al. GTPase activity regulates kinase activity and cellular phenotypes of parkinson's disease-associated LRRK2. Hum Mol Genet. 2013 Mar 15;22(6):1140-56.
13. Biskup S, Moore DJ, Celsi F, Higashi S, West AB, Andrabi SA, et al. Localization of LRRK2 to membranous and vesicular structures in mammalian brain. Ann Neurol. 2006 Nov;60(5):557-69.
14. Bonifati V. Shaking the genome: New studies reveal genetic risk for parkinson's disease. The Lancet Neurology. 2010;9(2):136-8.
15. Bozi M, Papadimitriou D, Antonellou R, Moraitou M, Maniati M, Vassilatis DK, et al. Genetic assessment of familial and early-onset parkinson's disease in a greek population. Eur J Neurol. 2013 Dec 7.
16. Braak H, Del Tredici K, Rub U, de Vos RA, Jansen Steur EN, Braak E. Staging of brain pathology related to sporadic parkinson's disease. Neurobiol Aging. 2003 Mar-Apr;24(2):197-211.
17. Brown TP, Rumsby PC, Capleton AC, Rushton L, Levy LS. Pesticides and parkinson's disease--is there a link? Environ Health Perspect. 2006 Feb;114(2):156-64.
18. Chan NC, Salazar AM, Pham AH, Sweredoski MJ, Kolawa NJ, Graham RL, et al. Broad activation of the ubiquitin-proteasome system by parkin is critical for mitophagy. Hum Mol Genet. 2011 May 1;20(9):1726-37.
19. Chang JW, Wachtel SR, Young D, Kang UJ. Biochemical and anatomical characterization of forepaw adjusting steps in rat models of parkinson's disease: Studies on medial forebrain bundle and striatal lesions. Neuroscience. 1999 Jan;88(2):617-28.
20. Chaudhuri KR, Healy DG, Schapira AH, National Institute for Clinical Excellence. Non-motor symptoms of parkinson's disease: Diagnosis and management. Lancet Neurol. 2006 Mar;5(3):235-45.
21. Chen CY, Weng YH, Chien KY, Lin KJ, Yeh TH, Cheng YP, et al. (G2019S) LRRK2 activates MKK4-JNK pathway and causes degeneration of SN dopaminergic neurons in a transgenic mouse model of PD. Cell Death Differ. 2012 Oct;19(10):1623-33.

22. Chen H, Burton EA, Ross GW, Huang X, Savica R, Abbott RD, et al. Research on the premotor symptoms of parkinson's disease: Clinical and etiological implications. Environ Health Perspect. 2013 Nov-Dec;121(11-12):1245-52.
23. Cho HJ, Liu G, Jin SM, Parisiadou L, Xie C, Yu J, et al. MicroRNA-205 regulates the expression of parkinson's disease-related leucine-rich repeat kinase 2 protein. Hum Mol Genet. 2013 Feb 1;22(3):608-20.
24. Chou JS, Chen CY, Chen YL, Weng YH, Yeh TH, Lu CS, et al. (G2019S) LRRK2 causes early-phase dysfunction of SNpc dopaminergic neurons and impairment of corticostriatal long-term depression in the PD transgenic mouse. Neurobiol Dis. 2014 May 14.
25. Cicchetti F, Lapointe N, Roberge-Tremblay A, Saint-Pierre M, Jimenez L, Ficke BW, et al. Systemic exposure to paraquat and maneb models early parkinson's disease in young adult rats. Neurobiol Dis. 2005 Nov;20(2):360-71.
26. Clark LN, Wang Y, Karlins E, Saito L, Mejia-Santana H, Harris J, et al. Frequency of LRRK2 mutations in early- and late-onset parkinson disease. Neurology. 2006 Nov 28;67(10):1786-91.
27. Collier TJ, Kanaan NM, Kordower JH. Ageing as a primary risk factor for parkinson's disease: Evidence from studies of non-human primates. Nature Reviews Neuroscience. 2011;12(6):359-66.
28. Cookson MR. The role of leucine-rich repeat kinase 2 (LRRK2) in parkinson's disease. Nat Rev Neurosci. 2010 Dec;11(12):791-7.
29. Costello S, Cockburn M, Bronstein J, Zhang X, Ritz B. Parkinson's disease and residential exposure to maneb and paraquat from agricultural applications in the central valley of california. Am J Epidemiol. 2009 Apr 15, 2009;169(8):919-26.
30. De Rosa A, De Michele G, Guacci A, Carbone R, Lieto M, Peluso S, et al. Genetic screening for the LRRK2 R1441C and G2019S mutations in parkinsonian patients from campania. J Parkinsons Dis. 2014;4(1):123-8.
31. Deng J, Lewis PA, Greggio E, Sluch E, Beilina A, Cookson MR. Structure of the ROC domain from the parkinson's disease-associated leucine-rich repeat kinase 2 reveals a dimeric GTPase. Proc Natl Acad Sci U S A. 2008 Feb 5;105(5):1499-504.

32. Desplats P, Patel P, Kosberg K, Mante M, Patrick C, Rockenstein E, et al. Combined exposure to maneb and paraquat alters transcriptional regulation of neurogenesis-related genes in mice models of parkinson's disease. Mol Neurodegener. 2012 Sep 28;7:49,1326-7-49.
33. Dexter DT, Jenner P. Parkinson disease: From pathology to molecular disease mechanisms. Free Radic Biol Med. 2013 Sep;62:132-44.
34. Di Fonzo A, Rohe CF, Ferreira J, Chien HF, Vacca L, Stocchi F, et al. A frequent LRRK2 gene mutation associated with autosomal dominant parkinson's disease. Lancet. 2005 Jan 29-Feb 4;365(9457):412-5.
35. Di Fonzo A, Tassorelli C, De Mari M, Chien HF, Ferreira J, Rohe CF, et al. Comprehensive analysis of the LRRK2 gene in sixty families with parkinson's disease. Eur J Hum Genet. 2006 Mar;14(3):322-31.
36. Doder M, Jahanshahi M, Turjanski N, Moseley IF, Lees AJ. Parkinson's syndrome after closed head injury: A single case report. Journal of Neurology, Neurosurgery & Psychiatry. 1999;66(3):380-5.
37. Dorval V, Mandemakers W, Jolivette F, Coudert L, Mazroui R, De Strooper B, et al. Gene and MicroRNA transcriptome analysis of parkinson's related LRRK2 mouse models. PLoS One. 2014 Jan 10;9(1):e85510.
38. Dranka BP, Gifford A, Ghosh A, Zielonka J, Joseph J, Kanthasamy AG, et al. Diapocynin prevents early parkinson's disease symptoms in the leucine-rich repeat kinase 2 (LRRK2(R1441G)) transgenic mouse. Neurosci Lett. 2013 Aug 9;549:57-62.
39. Drechsel DA, Patel M. Differential contribution of the mitochondrial respiratory chain complexes to reactive oxygen species production by redox cycling agents implicated in parkinsonism. Toxicol Sci. 2009 Dec;112(2):427-34.
40. Driver JA, Logroscino G, Gaziano JM, Kurth T. Incidence and remaining lifetime risk of parkinson disease in advanced age. Neurology. 2009;72(5):432-8.
41. Dusonchet J, Kochubey O, Stafa K, Young SM,Jr, Zufferey R, Moore DJ, et al. A rat model of progressive nigral neurodegeneration induced by the parkinson's disease-associated G2019S mutation in LRRK2. J Neurosci. 2011 Jan 19;31(3):907-12.
42. .Emre M. What causes mental dysfunction in parkinson's disease? Mov Disord. 2003 Sep;18 Suppl 6:S63-71.

43. Firestone JA, Smith-Weller T, Franklin G, Swanson P, Longstreth WT, Checkoway H. Pesticides and risk of parkinson disease: A population-based case-control study. Arch Neurol. 2005;62(1):91-5.
44. Fleming SM. Behavioral outcome measures for the assessment of sensorimotor function in animal models of movement disorders. Int Rev Neurobiol. 2009;89:57-65.
45. Fleming SM, Schallert T, Ciucci MR. Cranial and related sensorimotor impairments in rodent models of parkinson's disease. Behav Brain Res. 2012 Jun 1;231(2):317-22.
46. Funayama M, Hasegawa K, Ohta E, Kawashima N, Komiyama M, Kowa H, et al. An LRRK2 mutation as a cause for the parkinsonism in the original PARK8 family. Ann Neurol. 2005 Jun;57(6):918-21.
47. Galter D, Westerlund M, Carmine A, Lindqvist E, Sydow O, Olson L. LRRK2 expression linked to dopamine-innervated areas. Ann Neurol. 2006 Apr;59(4):714-9.
48. Gandhi PN, Wang X, Zhu X, Chen SG, Wilson-Delfosse AL. The roc domain of leucine-rich repeat kinase 2 is sufficient for interaction with microtubules. J Neurosci Res. 2008 Jun;86(8):1711-20.
49. Giesert F, Hofmann A, Burger A, Zerle J, Kloos K, Hafen U, et al. Expression analysis of Lrrk1, Lrrk2 and Lrrk2 splice variants in mice. PLoS One. 2013 May 10;8(5):e63778.
50. Gillardon F. Leucine-rich repeat kinase 2 phosphorylates brain tubulin-beta isoforms and modulates microtubule stability--a point of convergence in parkinsonian neurodegeneration? J Neurochem. 2009 Sep;110(5):1514-22.
51. Goldwurm S, Di Fonzo A, Simons EJ, Rohe CF, Zini M, Canesi M, et al. The G6055A (G2019S) mutation in LRRK2 is frequent in both early and late onset parkinson's disease and originates from a common ancestor. J Med Genet. 2005 Nov;42(11):e65.
52. Greggio E. Role of LRRK2 kinase activity in the pathogenesis of parkinson's disease. Biochem Soc Trans. 2012 Oct;40(5):1058-62.
53. Greggio E, Jain S, Kingsbury A, Bandopadhyay R, Lewis P, Kaganovich A, et al. Kinase activity is required for the toxic effects of mutant LRRK2/dardarin. Neurobiol Dis. 2006 Aug;23(2):329-41.
54. Greggio E, Zambrano I, Kaganovich A, Beilina A, Taymans JM, Daniels V, et al. The parkinson disease-associated leucine-rich repeat kinase 2 (LRRK2) is a dimer that

undergoes intramolecular autophosphorylation. J Biol Chem. 2008 Jun 13;283(24):16906-14.

55. Guo L, Gandhi PN, Wang W, Petersen RB, Wilson-Delfosse AL, Chen SG. The parkinson's disease-associated protein, leucine-rich repeat kinase 2 (LRRK2), is an authentic GTPase that stimulates kinase activity. Exp Cell Res. 2007 Oct 1;313(16):3658-70.
56. Healy DG, Falchi M, O'Sullivan SS, Bonifati V, Durr A, Bressman S, et al. Phenotype, genotype, and worldwide genetic penetrance of LRRK2-associated parkinson's disease: A case-control study. Lancet Neurol. 2008 Jul;7(7):583-90.
57. Heo HY, Park JM, Kim CH, Han BS, Kim KS, Seol W. LRRK2 enhances oxidative stress-induced neurotoxicity via its kinase activity. Exp Cell Res. 2010 Feb 15;316(4):649-56.
58. Higashi S, Biskup S, West AB, Trinkaus D, Dawson VL, Faull RL, et al. Localization of parkinson's disease-associated LRRK2 in normal and pathological human brain. Brain Res. 2007 Jun 25;1155:208-19.
59. Higashi S, Moore DJ, Colebrooke RE, Biskup S, Dawson VL, Arai H, et al. Expression and localization of parkinson's disease-associated leucine-rich repeat kinase 2 in the mouse brain. J Neurochem. 2007 Jan;100(2):368-81.
60. Hinkle KM, Yue M, Behrouz B, Dachsel JC, Lincoln SJ, Bowles EE, et al. LRRK2 knockout mice have an intact dopaminergic system but display alterations in exploratory and motor co-ordination behaviors. Mol Neurodegener. 2012 May 30;7:25,1326-7-25.
61. Hubble JP, Cao T, Hassanein RE, Neuberger JS, Koller WC. Risk factors for parkinson's disease. Neurology. 1993;43(9):1693-7.
62. Hutson CB, Lazo CR, Mortazavi F, Giza CC, Hovda D, Chesselet MF. Traumatic brain injury in adult rats causes progressive nigrostriatal dopaminergic cell loss and enhanced vulnerability to the pesticide paraquat. J Neurotrauma. 2011 Sep;28(9):1783-801.
63. Iaccarino C, Crosio C, Vitale C, Sanna G, Carri MT, Barone P. Apoptotic mechanisms in mutant LRRK2-mediated cell death. Hum Mol Genet. 2007 Jun 1;16(11):1319-26.

64. Imai Y, Gehrke S, Wang HQ, Takahashi R, Hasegawa K, Oota E, et al. Phosphorylation of 4E-BP by LRRK2 affects the maintenance of dopaminergic neurons in drosophila. EMBO J. 2008 Sep 17;27(18):2432-43.
65. Ito G, Okai T, Fujino G, Takeda K, Ichijo H, Katada T, et al. GTP binding is essential to the protein kinase activity of LRRK2, a causative gene product for familial parkinson's disease. Biochemistry. 2007 Feb 6;46(5):1380-8.
66. Kim J, Lee J, Kim HJ, Kim JS, Shin E, Cho J, et al. The LRRK2 G2385R variant is a risk factor for sporadic parkinson's disease in the korean population. Parkinsonism Relat Disord. 2010;16(2):85-8.
67. Komatsu M, Waguri S, Chiba T, Murata S, Iwata J, Tanida I, et al. Loss of autophagy in the central nervous system causes neurodegeneration in mice. Nature. 2006 Jun 15;441(7095):880-4.
68. Kumar A, Ahmad I, Shukla S, Singh BK, Patel DK, Pandey HP, et al. Effect of zinc and paraquat co-exposure on neurodegeneration: Modulation of oxidative stress and expression of metallothioneins, toxicant responsive and transporter genes in rats. Free Radic Res. 2010 Aug;44(8):950-65.
69. Landers MR, Kinney JW, van Breukelen F. Forced exercise before or after induction of 6-OHDA-mediated nigrostriatal insult does not mitigate behavioral asymmetry in a hemiparkinsonian rat model. Brain Res. 2014 Jan 16;1543:263-70.
70. Langston JW, Ballard P, Tetrud JW, Irwin I. Chronic parkinsonism in humans due to a product of meperidine-analog synthesis. Science. 1983 Feb 25;219(4587):979-80.
71. Langston JW. The parkinson's complex: Parkinsonism is just the tip of the iceberg. Ann Neurol. 2006 Apr;59(4):591-6.
72. Law BM, Spain VA, Leinster VH, Chia R, Beilina A, Cho HJ, et al. A direct interaction between leucine-rich repeat kinase 2 and specific beta-tubulin isoforms regulates tubulin acetylation. J Biol Chem. 2014 Jan 10;289(2):895-908.
73. Lee P, Bordelon Y, Bronstein J, Ritz B. Traumatic brain injury, paraquat exposure, and their relationship to parkinson disease. Neurology. 2012;79(20):2061-6.
74. Lee Y, Dawson VL, Dawson TM. Animal models of parkinson's disease: Vertebrate genetics. Cold Spring Harb Perspect Med. 2012 Oct 1;2(10):10.1101/cshperspect.a009324.

75. Lee BD, Shin JH, VanKampen J, Petrucelli L, West AB, Ko HS, et al. Inhibitors of leucine-rich repeat kinase-2 protect against models of parkinson's disease. Nat Med. 2010 Sep;16(9):998-1000.
76. Li X, Patel JC, Wang J, Avshalumov MV, Nicholson C, Buxbaum JD, et al. Enhanced striatal dopamine transmission and motor performance with LRRK2 overexpression in mice is eliminated by familial parkinson's disease mutation G2019S. J Neurosci. 2010 Feb 3;30(5):1788-97.
77. Li X, Tan YC, Poulose S, Olanow CW, Huang XY, Yue Z. Leucine-rich repeat kinase 2 (LRRK2)/PARK8 possesses GTPase activity that is altered in familial parkinson's disease R1441C/G mutants. J Neurochem. 2007 Oct;103(1):238-47.
78. Li Y, Liu W, Oo TF, Wang L, Tang Y, Jackson-Lewis V, et al. Mutant LRRK2(R1441G) BAC transgenic mice recapitulate cardinal features of parkinson's disease. Nat Neurosci. 2009 Jul;12(7):826-8.
79. Liew Z, Wang A, Bronstein J, Ritz B. Job exposure matrix (JEM)-derived estimates of lifetime occupational pesticide exposure and the risk of parkinson's disease. Arch Environ Occup Health. 2014;69(4):241-51.
80. Liao J, Wu CX, Burlak C, Zhang S, Sahm H, Wang M, et al. Parkinson disease-associated mutation R1441H in LRRK2 prolongs the "active state" of its GTPase domain. Proc Natl Acad Sci U S A. 2014 Mar 18;111(11):4055-60.
81. Lin CH, Tsai PI, Wu RM, Chien CT. LRRK2 G2019S mutation induces dendrite degeneration through mislocalization and phosphorylation of tau by recruiting autoactivated GSK3ss. J Neurosci. 2010 Sep 29;30(39):13138-49.
82. Liu M, Dobson B, Glicksman MA, Yue Z, Stein RL. Kinetic mechanistic studies of wild-type leucine-rich repeat kinase 2: Characterization of the kinase and GTPase activities. Biochemistry. 2010 Mar 9;49(9):2008-17.
83. MacLeod D, Dowman J, Hammond R, Leete T, Inoue K, Abeliovich A. The familial parkinsonism gene LRRK2 regulates neurite process morphology. Neuron. 2006 Nov 22;52(4):587-93.
84. Maher NE, Golbe LI, Lazzarini AM, Mark MH, Currie LJ, Wooten GF, et al. Epidemiologic study of 203 sibling pairs with parkinson's disease: The GenePD study. Neurology. 2002;58(1):79-84.

85. Manzoni C, Mamais A, Dihanich S, McGoldrick P, Devine MJ, Zerle J, et al. Pathogenic parkinson's disease mutations across the functional domains of LRRK2 alter the autophagic/lysosomal response to starvation. Biochem Biophys Res Commun. 2013 Nov 29;441(4):862-6.
86. Matsumoto H, Noro H, Kaneshige Y, Chiba S, Miyano N, Motoi Y, et al. A correlation study between blink reflex habituation and clinical state in patients with parkinson's disease. J Neurol Sci. 1992 Feb;107(2):155-9.
87. Melrose HL, Dachsel JC, Behrouz B, Lincoln SJ, Yue M, Hinkle KM, et al. Impaired dopaminergic neurotransmission and microtubule-associated protein tau alterations in human LRRK2 transgenic mice. Neurobiol Dis. 2010 Dec;40(3):503-17.
88. Melrose HL, Kent CB, Taylor JP, Dachsel JC, Hinkle KM, Lincoln SJ, et al. A comparative analysis of leucine-rich repeat kinase 2 (Lrrk2) expression in mouse brain and lewy body disease. Neuroscience. 2007 Jul 29;147(4):1047-58.
89. Meylan E, Tschopp J. The RIP kinases: Crucial integrators of cellular stress. Trends Biochem Sci. 2005 Mar;30(3):151-9.
90. Miklossy J, Arai T, Guo JP, Klegeris A, Yu S, McGeer EG, et al. LRRK2 expression in normal and pathologic human brain and in human cell lines. J Neuropathol Exp Neurol. 2006 Oct;65(10):953-63.
91. Miyoshi E, Wietzikoski S, Camplessei M, Silveira R, Takahashi RN, Da Cunha C. Impaired learning in a spatial working memory version and in a cued version of the water maze in rats with MPTP-induced mesencephalic dopaminergic lesions. Brain Res Bull. 2002 May;58(1):41-7.
92. Muda K, Bertinetti D, Gesellchen F, Hermann JS, von Zweydorf F, Geerlof A, et al. Parkinson-related LRRK2 mutation R1441C/G/H impairs PKA phosphorylation of LRRK2 and disrupts its interaction with 14-3-3. Proc Natl Acad Sci U S A. 2014 Jan 7;111(1):E34-43.
93. Ng CH, Mok SZ, Koh C, Ouyang X, Fivaz ML, Tan EK, et al. Parkin protects against LRRK2 G2019S mutant-induced dopaminergic neurodegeneration in drosophila. J Neurosci. 2009 Sep 9;29(36):11257-62.

94. Nguyen HN, Byers B, Cord B, Shcheglovitov A, Byrne J, Gujar P, et al. LRRK2 mutant iPSC-derived DA neurons demonstrate increased susceptibility to oxidative stress. Cell Stem Cell. 2011 Mar 4;8(3):267-80.
95. Niu J, Yu M, Wang C, Xu Z. Leucine-rich repeat kinase 2 disturbs mitochondrial dynamics via dynamin-like protein. J Neurochem. 2012 Aug;122(3):650-8.
96. Olsson M, Nikkhah G, Bentlage C, Bjorklund A. Forelimb akinesia in the rat parkinson model: Differential effects of dopamine agonists and nigral transplants as assessed by a new stepping test. J Neurosci. 1995 May;15(5 Pt 2):3863-75.
97. Ossowska K, Smialowska M, Kuter K, Wieronska J, Zieba B, Wardas J, et al. Degeneration of dopaminergic mesocortical neurons and activation of compensatory processes induced by a long-term paraquat administration in rats: Implications for parkinson's disease. Neuroscience. 2006 Sep 15;141(4):2155-65.
98. Paisan-Ruiz C, Jain S, Evans EW, Gilks WP, Simon J, van der Brug M, et al. Cloning of the gene containing mutations that cause PARK8-linked parkinson's disease. Neuron. 2004 Nov 18;44(4):595-600.
99. Pan J, Li H, Wang Y, Ma J, Zhang J, Wang G, et al. Fibroblast growth factor 20 (FGF20) polymorphism is a risk factor for Parkinson’s disease in chinese population. Parkinsonism Relat Disord. 2012;18(5):629-31.
100. Parisiadou L, Xie C, Cho HJ, Lin X, Gu XL, Long CX, et al. Phosphorylation of ezrin/radixin/moesin proteins by LRRK2 promotes the rearrangement of actin cytoskeleton in neuronal morphogenesis. J Neurosci. 2009 Nov 4;29(44):13971-80.
101. Peng J, Mao XO, Stevenson FF, Hsu M, Andersen JK. The herbicide paraquat induces dopaminergic nigral apoptosis through sustained activation of the JNK pathway. J Biol Chem. 2004 Jul 30;279(31):32626-32.
102. Peng J, Oo ML, Andersen JK. Synergistic effects of environmental risk factors and gene mutations in Parkinson’s disease accelerate age-related neurodegeneration. J Neurochem. 2010;115(6):1363-73.
103. Peng J, Peng L, Stevenson FF, Doctrow SR, Andersen JK. Iron and paraquat as synergistic environmental risk factors in sporadic parkinson's disease accelerate age-related neurodegeneration. The Journal of Neuroscience. 2007;27(26):6914-22.

104. Pereira C, Miguel Martins L, Saraiva L. LRRK2, but not pathogenic mutants, protects against H2O2 stress depending on mitochondrial function and endocytosis in a yeast model. Biochim Biophys Acta. 2014 Jun;1840(6):2025-31.

105. Pezzoli G, Cereda E. Exposure to pesticides or solvents and risk of parkinson disease. Neurology. 2013 May 28;80(22):2035-41.

106. Phillipson OT. Management of the aging risk factor for Parkinson's disease. Neurobiol Aging. 2014;35(4):847-57.

107. Plowey ED, Cherra SJ,3rd, Liu YJ, Chu CT. Role of autophagy in G2019S-LRRK2-associated neurite shortening in differentiated SH-SY5Y cells. J Neurochem. 2008 May;105(3):1048-56.

108. Pungaliya PP, Bai Y, Lipinski K, Anand VS, Sen S, Brown EL, et al. Identification and characterization of a leucine-rich repeat kinase 2 (LRRK2) consensus phosphorylation motif. PLoS One. 2010 Oct 27;5(10):e13672.

109. Quinn R. Comparing rat's to human's age: How old is my rat in people years? Nutrition. 2005 Jun;21(6):775-7.

110. Ramonet D, Daher JP, Lin BM, Stafa K, Kim J, Banerjee R, et al. Dopaminergic neuronal loss, reduced neurite complexity and autophagic abnormalities in transgenic mice expressing G2019S mutant LRRK2. PLoS One. 2011 Apr 6;6(4):e18568.

111. Rappold PM, Cui M, Chesser AS, Tibbett J, Grima JC, Duan L, et al. Paraquat neurotoxicity is mediated by the dopamine transporter and organic cation transporter-3. PNAS Proceedings of the National Academy of Sciences of the United States of America. 2011;108(51):20766-71.

112. Ray A, Martinez BA, Berkowitz LA, Caldwell GA, Caldwell KA. Mitochondrial dysfunction, oxidative stress, and neurodegeneration elicited by a bacterial metabolite in a C. elegans parkinson's model. Cell Death Dis. 2014 Jan 9;5:e984.

113. Ray S, Bender S, Kang S, Lin R, Glicksman MA, Liu M. The parkinson disease-linked LRRK2 protein mutation I2020T stabilizes an active state conformation leading to increased kinase activity. J Biol Chem. 2014 May 9;289(19):13042-53.

114. Ritz BR, Manthripragada AD, Costello S, Lincoln SJ, Farrer MJ, Cockburn M, et al. Dopamine transporter genetic variants and pesticides in parkinson's disease. Environ Health Perspect. 2009 Jun;117(6):964-9.

115. Ross OA, Wu Y, Lee M, Funayama M, Chen M, Soto AI, et al. Analysis of Lrrk2 R1628P as a risk factor for parkinson's disease. Ann Neurol. 2008;64(1):88-92.

116. Ruiz-Martinez J, de la Riva P, Rodriguez-Oroz MC, Mondragon Rezola E, Bergareche A, Gorostidi A, et al. Prevalence of cancer in parkinson's disease related to R1441G and G2019S mutations in LRRK2. Mov Disord. 2014 May;29(6):750-5.

117. Saaksjarvi K, Knekt P, Rissanen H, Laaksonen MA, Reunanen A, Mannisto S. Prospective study of coffee consumption and risk of parkinson's disease. Eur J Clin Nutr. 2008 Jul;62(7):908-15.

118. Saha S, Liu-Yesucevitz L, Wolozin B. Regulation of autophagy by LRRK2 in caenorhabditis elegans. Neurodegener Dis. 2014;13(2-3):110-3.

119. Santpere G, Ferrer I. LRRK2 and neurodegeneration. Acta Neuropathol. 2009 Mar;117(3):227-46.

120. Schapansky J, Nardozzi JD, Felizia F, Lavoie MJ. Membrane recruitment of endogenous LRRK2 precedes its potent regulation of autophagy. Hum Mol Genet. 2014 Apr 15.

121. Schneider SA, Obeso JA. Clinical and pathological features of parkinson's disease. Curr Top Behav Neurosci. 2014 May 22.

122. Seki N, Takahashi Y, Tomiyama H, Rogaeva E, Murayama S, Mizuno Y, et al. Comprehensive mutational analysis of LRRK2 reveals variants supporting association with autosomal dominant parkinson's disease. J Hum Genet. 2011 Sep;56(9):671-5.

123. Sepulveda B, Mesias R, Li X, Yue Z, Benson DL. Short- and long-term effects of LRRK2 on axon and dendrite growth. PLoS One. 2013 Apr 30;8(4):e61986.

124. Sharma S, Bandopadhyay R, Lashley T, Renton AE, Kingsbury AE, Kumaran R, et al. LRRK2 expression in idiopathic and G2019S positive parkinson's disease subjects: A morphological and quantitative study. Neuropathol Appl Neurobiol. 2011 Dec;37(7):777-90.

125. Shimizu K, Ohtaki K, Matsubara K, Aoyama K, Uezono T, Saito O, et al. Carrier-mediated processes in blood--brain barrier penetration and neural uptake of paraquat. Brain Res. 2001 Jul 6;906(1-2):135-42.

126. Simon-Sanchez J, Herranz-Perez V, Olucha-Bordonau F, Perez-Tur J. LRRK2 is expressed in areas affected by parkinson's disease in the adult mouse brain. Eur J Neurosci. 2006 Feb;23(3):659-66.

127. Singhal NK, Srivastava G, Patel DK, Jain SK, Singh MP. Melatonin or silymarin reduces maneb- and paraquat-induced parkinson's disease phenotype in the mouse. J Pineal Res. 2011 Mar;50(2):97-109.

128. Smith WW, Pei Z, Jiang H, Dawson VL, Dawson TM, Ross CA. Kinase activity of mutant LRRK2 mediates neuronal toxicity. Nat Neurosci. 2006 Oct;9(10):1231-3.

129. Somayajulu-Nitu M, Sandhu JK, Cohen J, Sikorska M, Sridhar TS, Matei A, et al. Paraquat induces oxidative stress, neuronal loss in substantia nigra region and parkinsonism in adult rats: Neuroprotection and amelioration of symptoms by water-soluble formulation of coenzyme Q10. BMC Neurosci. 2009 Jul 27;10:88,2202-10-88.

130. Sulzer D. Multiple hit hypotheses for dopamine neuron loss in parkinson's disease. Trends Neurosci. 2007 5;30(5):244-50.

131. Tanner CM, Kamel F, Ross GW, Hoppin JA, Goldman SM, Korell M, et al. Rotenone, paraquat, and parkinson's disease. Environ Health Perspect. 2011 Jun 2011;119(6):866-72.

132. Taymans JM, Van den Haute C, Baekelandt V. Distribution of PINK1 and LRRK2 in rat and mouse brain. J Neurochem. 2006 Aug;98(3):951-61.

133. Thiruchelvam M, McCormack A, Richfield EK, Baggs RB, Tank AW, di Monte DA, et al. Age-related irreversible progressive nigrostriatal dopaminergic neurotoxicity in the paraquat and maneb model of the parkinson's disease phenotype. Eur J Neurosci. 2003;18(3):589-600.

134. Toft M, Mata IF, Kachergus JM, Ross OA, Farrer MJ. LRRK2 mutations and parkinsonism. Lancet. 2005 Apr 2-8;365(9466):1229-30.

135. Tong Y, Pisani A, Martella G, Karouani M, Yamaguchi H, Pothos EN, et al. R1441C mutation in LRRK2 impairs dopaminergic neurotransmission in mice. Proc Natl Acad Sci U S A. 2009 Aug 25;106(34):14622-7.

136. Tong Y, Yamaguchi H, Giaime E, Boyle S, Kopan R, Kelleher RJ,3rd, et al. Loss of leucine-rich repeat kinase 2 causes impairment of protein degradation pathways,

accumulation of alpha-synuclein, and apoptotic cell death in aged mice. Proc Natl Acad Sci U S A. 2010 May 25;107(21):9879-84.

137. Tsika E, Moore DJ. Contribution of GTPase activity to LRRK2-associated parkinson disease. Small GTPases. 2013 Jul-Sep;4(3):164-70.

138. Tsika E, Moore DJ. Mechanisms of LRRK2-mediated neurodegeneration. Curr Neurol Neurosci Rep. 2012 Jun;12(3):251-60.

139. Typlt M, Mirkowski M, Azzopardi E, Ruettiger L, Ruth P, Schmid S. Mice with deficient BK channel function show impaired prepulse inhibition and spatial learning, but normal working and spatial reference memory. PLoS One. 2013 Nov 26;8(11):e81270.

140. van der Mark M, Nijssen PC, Vlaanderen J, Huss A, Mulleners WM, Sas AM, et al. A case-control study of the protective effect of alcohol, coffee, and cigarette consumption on parkinson disease risk: Time-since-cessation modifies the effect of tobacco smoking. PLoS One. 2014 Apr 30;9(4):e95297.

141. Venderova K, Kabbach G, Abdel-Messih E, Zhang Y, Parks RJ, Imai Y, et al. Leucine-rich repeat kinase 2 interacts with parkin, DJ-1 and PINK-1 in a drosophila melanogaster model of parkinson's disease. Hum Mol Genet. 2009 Nov 15;18(22):4390-404.

142. Vitte J, Traver S, Maues De Paula A, Lesage S, Rovelli G, Corti O, et al. Leucine-rich repeat kinase 2 is associated with the endoplasmic reticulum in dopaminergic neurons and accumulates in the core of lewy bodies in parkinson disease. J Neuropathol Exp Neurol. 2010 Sep;69(9):959-72.

143. Wang X, Yan MH, Fujioka H, Liu J, Wilson-Delfosse A, Chen SG, et al. LRRK2 regulates mitochondrial dynamics and function through direct interaction with DLP1. Hum Mol Genet. 2012 May 1;21(9):1931-44.

144. West AB, Moore DJ, Choi C, Andrabi SA, Li X, Dikeman D, et al. Parkinson's disease-associated mutations in LRRK2 link enhanced GTP-binding and kinase activities to neuronal toxicity. Hum Mol Genet. 2007 Jan 15;16(2):223-32.

145. Westerlund M, Belin AC, Anvret A, Bickford P, Olson L, Galter D. Developmental regulation of leucine-rich repeat kinase 1 and 2 expression in the brain

and other rodent and human organs: Implications for parkinson's disease. Neuroscience. 2008 Mar 18;152(2):429-36.

146. Williams-Gray CH, Foltynie T, Lewis SJG, Barker RA. Cognitive deficits and psychosis in parkinson's disease: A review of pathophysiology and therapeutic options. CNS Drugs. 2006;20(6):477-505.

147. Wills J, Credle J, Oaks AW, Duka V, Lee JH, Jones J, et al. Paraquat, but not maneb, induces synucleinopathy and tauopathy in striata of mice through inhibition of proteasomal and autophagic pathways. PLoS One. 2012;7(1):e30745.

148. Winner B, Melrose HL, Zhao C, Hinkle KM, Yue M, Kent C, et al. Adult neurogenesis and neurite outgrowth are impaired in LRRK2 G2019S mice. Neurobiol Dis. 2011 Mar;41(3):706-16.

149. Woodlee MT, Asseo-Garcia AM, Zhao X, Liu SJ, Jones TA, Schallert T. Testing forelimb placing "across the midline" reveals distinct, lesion-dependent patterns of recovery in rats. Exp Neurol. 2005 Feb;191(2):310-7.

150. Yao C, El Khoury R, Wang W, Byrd TA, Pehek EA, Thacker C, et al. LRRK2-mediated neurodegeneration and dysfunction of dopaminergic neurons in a caenorhabditis elegans model of parkinson's disease. Neurobiol Dis. 2010 Oct;40(1):73-81.

151. Zhang D, Jiang H, Xie J. Alcohol intake and risk of parkinson's disease: A meta-analysis of observational studies. Mov Disord. 2014 May;29(6):819-22.

152. Zhang Z, Burgunder JM, An X, Wu Y, Chen W, Zhang J, et al. LRRK2 R1628P variant is a risk factor of parkinson's disease among han-chinese from mainland china. Mov Disord. 2009 Oct 15;24(13):1902-5.

153. Zhou H, Huang C, Tong J, Hong WC, Liu YJ, Xia XG. Temporal expression of mutant LRRK2 in adult rats impairs dopamine reuptake. Int J Biol Sci. 2011;7(6):753-61.

154. Zimprich A, Biskup S, Leitner P, Lichtner P, Farrer M, Lincoln S, et al. Mutations in LRRK2 cause autosomal-dominant parkinsonism with pleomorphic pathology. Neuron. 2004 Nov 18;44(4):601-7.

155. Zoetmulder M, Biernat HB, Nikolic M, Korbo L, Friberg L, Jennum PJ. Prepulse inhibition is associated with attention, processing speed, and 123I-FP-CIT SPECT in parkinson's disease. J Parkinsons Dis. 2014;4(1):77-87.

Curriculum Vitae

Komal Shaikh

Education

2012-2014 University of Western Ontario
MSc. – Neuroscience

Thesis Project: Investigating cognitive and motor abilities of a LRRK2 rat model of Parkinson Disease. *Advisor: Dr. Susanne Schmid*

2008-2012 University of Western Ontario
BSc. – Double Major in Psychology and Physiology

Research

Publications

Shaikh, K.T., Schmid, S. (2013). *Gender differences in modulations of acoustic startle response in Sprague Dawley rats.* Western Undergraduate Research Journal. [Accepted – Awaiting Publication]

Poster Presentations

Shaikh, K.T., Youshin, K., Yang, A., Kwok, J., Schmid, S. (2014, May). *Investigating the Multiple Hit Hypothesis of Parkinson disease.* Poster presented at the Southern Ontario Neuroscience Association 34th Annual Meeting, London, Ontario, Canada.

Yang, A., **Shaikh, K.T.**, Youshin, K., Kwok, J., Schmid, S. (2014, May). *Cognitive deficits in a transgenic rat model of Parkinson disease.* Poster presented at the Southern Ontario Neuroscience Association 34th Annual Meeting, London, Ontario, Canada.

Shaikh, K.T., Kwok, J., Youshin, K., Yang, A., Schmid, S. (2014, March). *Investigating the Multiple Hit Hypothesis of Parkinson disease.* Poster presented at the London Health Research Day, London, Ontario, Canada.

Shaikh, K.T., Schmid, S. (2013, October). *Lessons from a transgenic model of familial Parkinson disease*. Poster presented at 20th Annual Murray Barr Research Day, London, ON, Canada.

Shaikh, K.T., Schmid, S. (2013, September). *Behavioural analysis of a transgenic LRRK2 rat model of Parkinson disease.* Poster presented at the Grand Challenges in Parkinson Disease Conference, Grand Rapids, Michigan, United States of America.

Shaikh, K.T., Yang, A., Barros, W., Walewski, C., Schmid, S. (2013, May). *Motor and cognitive abilities of a transgenic LRRK2 rat model of Parkinson disease.* Poster presented at the Canadian Association for Neuroscience 7th Annual Meeting, Toronto, Ontario, Canada.

Shaikh, K.T., Yang, A., Barros, W., Walewski, C., Schmid, S. (2013, May). *Exploring a transgenic LRRK2 rat model of Parkinson disease.* Poster presented at the Southern Ontario Neuroscience Association 33rd Annual Meeting, Waterloo, Ontario, Canada.

Shaikh, K.T., Walewski, C., Yang, A., Schmid, S. (2013, March). *Motor characteristics of a transgenic LRRK2 rat model of Parkinson disease.* Poster presented at the London Health Research Day, London, Ontario, Canada.

Barros, W., **Shaikh, K.T.**, Schmid, S. (2013, March). *Cognitive characteristics of a transgenic LRRK2 rat model of Parkinson disease.* Poster presented at the London Health Research Day, London, Ontario, Canada.

Shaikh, K.T., Walewski, C., Yang, A., Schmid, S. (2013, March). *Investigating a transgenic LRRK2 rat model of Parkinson disease.* Poster presented at the Western Research Forum, London, Ontario, Canada.

Barros, W., **Shaikh, K.T.**, Schmid, S. (2013, March). *Cognitive abilities of a transgenic LRRK2 rat model of Parkinson disease.* Poster presented at the Western Research Forum, London, Ontario, Canada.

Shaikh, K.T., Schmid, S. (2011, April). *Gender differences in modulations of acoustic startle response in Sprague Dawley rats.* Poster presented at the Ontario Undergraduate Neuroscience Conference, Hamilton, Ontario, Canada.

Shaikh, K.T., Schmid, S. (2011, May). *Gender differences in modulations of acoustic startle response in Sprague Dawley rats.* Poster presented at the 31st annual meeting of the Southern Ontario Neuroscience Association, Guelph, Ontario, Canada.

Conference Talks

Shaikh, K.T., Schmid, S. (2011, March). *Gender differences in modulations of acoustic startle response in Sprague Dawley rats.* Symposium Presentation, Western Undergraduate Research Forum, London, Ontario, Canada.

Honors & Awards

- Ontario Graduate Scholarship 2014-2015
- Grand Challenges in Parkinson Disease Conference – 1st Place Poster Competition 2013
- Western Research Forum – 1st Place Poster Competition 2013
- Western Graduate Research Scholarship 2012-2014
- University of Western Ontario – Continuing Scholarship 2008

- Governor General's Academic Medal 2008
- Canadian Federation of University Women Scholarship 2008
- The University of Toronto National Book Award 2008
- The Linscott Scholarship 2008

Research Training

Sept 08 – April 12 University of Western Ontario [London, Ontario]
Research Assistant, Schmid Lab, Neurobiology

- Researched the mechanisms of acoustic startle modulations
- Observed and practiced several lab techniques, including rodent brain slicing, brain mapping, and analyzing behavioural responses

Sept 11- April 12 University of Western Ontario [London, Ontario]
Research Assistant, Zarbatany Lab, Developmental Psychology

- Investigated the effect of peer group relations on children's psychological adjustment
- Determined positive affect in children as a function of their social status

May 10 – Sept 10 Ottawa Hospital Research Institute [Ottawa, Ontario]
Research Assistant, Kothary Lab, Regenerative Medicine

- Investigated muscular defects of spinal muscular atrophy through the isolation of tibialis anterior muscle in mice
- Practiced several lab techniques, including PCR, genotyping, and dissection

Professional Service

Teaching Experience

Sept 12-May 12; *Teaching Assistant* – Integrative Neuroscience Course (ACB4511)
Sept 13- Jan 14 University of Western Ontario

- Graded course work, as well as assisted students with course relevant material and assignments

Clinical Experience

May 14 - Sept 14 Intensive Behaviour Intervention – Thames Valley Children's Centre
Junior Therapist

- Taught basic skills to an autistic child in a direct one-on-one approach using Applied Behaviour Analysis principles

May 13- April 14 Intensive Multi-Treatment Intervention Program
Play Therapy Volunteer

- Provided play therapy for an autistic child, focusing on increasing social behaviours through a cognitive behavioural approach